Renewable and Sustainable Energy Reviews 144 (2021) 111068

Contents lists available at ScienceDirect

Renewable and Sustainable Energy Reviews

journal homepage: http://www.elsevier.com/locate/rser

Sludge-derived biochars: A review on the influence of synthesis conditions on pollutants removal efficiency from wastewaters

Salah Jellali [a,*], Besma Khiari [b], Muhammad Usman [a], Helmi Hamdi [c], Yassine Charabi [a], Mejdi Jeguirim [d]

[a] PEIE Research Chair for the Development of Industrial Estates and Free Zones, Center for Environmental Studies and Research, Sultan Qaboos University, Al-Khoud 123, Muscat, Oman
[b] Wastewaters and Environment Laboratory, Water Research and Technologies Center (CERTE), Technopark Borj Cedria, University of Carthage, P.O.Box 273, Soliman, 8020, Tunisia
[c] Center for Sustainable Development, College of Arts and Sciences, Qatar University, P.O. Box 2713, Doha, Qatar
[d] Institut de Science des Matériaux de Mulhouse, 15, Rue Jean Starcky, 68057, Mulhouse Cedex, France

ARTICLE INFO

Keywords:
Sludge
Pyrolysis
Biochar
Wastewater treatment
Pollutant adsorption

ABSTRACT

Pyrolysis is a thermochemical process that permits the conversion of biomasses into energy (bio-oil and biogas) and a solid residue called biochar. The generation of biochar from lignocellulosic materials has been, for long-time, the predominant research focus. Wastewater treatment plants produce huge amounts of sludge biomass and there exists an increasing evidence for their possible reuse as a promising pyrolysis feedstock in recent literature. Though the valorization of biochars generated from lignocellulosic biomasses has been the subject of many reviews, there exists a critical knowledge gap regarding the effect of synthesis conditions of the sludge-derived biochars (SDBs) on their efficiency in the treatment of wastewater. This review critically analyzes the available literature related to SDBs characteristics and application to adsorb inorganic and organic pollutants from effluents. The physico-chemical properties and adsorption efficiency of SDBs are mainly tuned by the nature of raw sludge, pyrolysis conditions, and pre/post-treatments. Indeed, biochars originating from digested sludge have better adsorption capacities towards nutrients and heavy metals compared to those obtained from the non-digested sludge. The nutrients recovery from urban wastewater could be significantly improved when the raw sludge is mixed with lignocellulosic biomass and Mg/Ca rich materials. On the other hand, the chemical activation of sludge at reagent/sludge ratios higher than 2:1 permits to generate SDBs with adsorption capacities comparable and even better than commercial activated carbons. Moreover, the embedment/coating of SDBs with specific nanomaterials and tailored functional groups could significantly improve the adsorption capacities of various organic toxic pollutants and at the same time enhance their chemical degradation. The effect of the nature of target pollutants (organic or inorganic) on the underlying adsorption mechanisms by SDBs was also deeply reviewed. Finally, this paper provides the main application challenges as well as insights regarding the promising future directions for SDBs research and development.

1. Introduction

The worldwide population has significantly increased from 3 billion in 1960 to 7.7 billion in mid-2019. It is expected to reach 10.1 billion in 2050 [1]. This population increase is systematically accompanied by an important food and water consumption and, therefore, a proportional generation of sludge from wastewater treatment plants (WWTPs). Global production of sewage sludge has been estimated to about 45 million dry tons per year. Depending on the quality of the influent in WWTPs, sludge may contain several harmful inorganic and organic substances (such as heavy metals, pharmaceuticals and pathogens) as well as beneficial compounds including organic matter, and macro- and micro-nutrients [2,3]. Considering safety requirements and circular economy exigencies, the sustainable management of sludge represents a serious environmental concern and a real challenge/opportunity for all the concerned stakeholders [2].

Different technologies have been explored to reduce the risks

* Corresponding author.
E-mail addresses: s.jellali@squ.edu.om (S. Jellali), besmakhiari@yahoo.com (B. Khiari), muhammad.usman@squ.edu.om (M. Usman), hhamdi@qu.edu.qa (H. Hamdi), yassine@squ.edu.om (Y. Charabi), mejdi.jeguirim@uha.fr (M. Jeguirim).

https://doi.org/10.1016/j.rser.2021.111068
Received 21 June 2020; Received in revised form 11 March 2021; Accepted 1 April 2021
Available online 8 April 2021
1364-0321/

Abbreviation list/nomenclature

ADS	Anaerobically digested sludge
A-SDBs	Aerobic sludge derived biochar
AN-SDBs	Anaerobic sludge derived biochar
C	Polluant initial concentration (mg L^{-1})
C_e	Pollutant concentration at equilibrium (mg L^{-1})
CEC	Cation Exchange Capacity (cmol kg^{-1})
D	SDB dose (g L^{-1})
DS	Dewatered sludge
DDS	Dewatered digested sludge
EMI	Electromagnetic Induction Method
FTIR	Fourier-transform infrared spectroscopy
G	Heating rate or pyrolysis gradient temperature (°C min^{-1})
ICP	Inductively Coupled Plasma
k_1	Equilibrium rate constant of pseudo-first-order adsorption (min^{-1})
k_2	Pseudo-second-order rate constant of adsorption (mg g^{-1} min^{-1})
K_f	Freundlich constant (L/mg)
K_L	Langmuir constant (L/mg)
NMR	Nuclear Magnetic Resonance
MSSDB	Mixture Sludge-Starch-Derived-Biochar
n_F	Freundlich equation exponent
NCC	Nano-composite coating
PCA	Physico-chemical activation
PFO	Pseudo-first-order model
PSO	Pseudo-second-order model
PS	Petrochemistry sludge
PZC	Point of zero charge
q_e	Amount of pollutant adsorbed at equilibrium (mg g^{-1})
$q_{e,I}$	Pollutant adsorbed amount at equilibrium predicted by the pseudo-first-order model
$q_{e,II}$	Pollutant adsorbed amount at equilibrium predicted by the pseudo-second-order model
q_{max}	Maximum adsorption capacity of the adsorbent (mg g^{-1})
q_t	Adsorbed pollutant amount at time t (mg g^{-1})
RSM	Response surface methodology
SA or SSA	Specific Surface Area (m^2/g)
SEM/EDX	Scanning Electron Microscopy (SEM) with Energy Dispersive X-Ray (EDX)
SDB	Sewage derived biochar
t	Residence time (s, min or h)
T	Final pyrolysis temperature (K or °C)
TE	Treatment effluent
V_t	Total pore volume (cm^3 g^{-1})
WAS	Waste activated sludge
WS	Walnut shells
WWTP	Waste water treatment plant
XPS	X-ray photoelectron spectroscopy
XRD	X-ray diffraction
Y	Char yield (%)

associated with sludge reuse in order to benefit from its constituents. These technologies include: i) agricultural valorization as organic amendments [3,4], ii) anaerobic digestion to produce biogas (mainly methane) and nutrient-rich digestate for energy and agronomic purposes, respectively [5], iii) reuse as low cost materials in building construction [6], and iv) thermochemical conversion through combustion or gasification for energy and biofuel production [7]. Unfortunately, these techniques present drawbacks such as bad smells, relatively low output, dependency to micro-organisms, pollutant release, etc. On the contrary, pyrolysis, which is a thermo-chemical conversion method that occurs in absence of oxygen at relatively lower temperatures, is more advantageous. It converts sludge into fuels (bio-oil and gas) for energy purposes and solid residues named biochars. Even though the bio-oil has interesting energy content, it should be handled with precaution as it could be corrosive and/or contain hazardous compounds [8]. The SDBs could be valorized in various applications including energy production, agriculture and wastewater treatment.

Particular attention has been paid during the last decade to the reuse of biochars for the removal of chemical contaminants from aqueous solutions. The recent growing interest in SDBs could be attributed to the promising results regarding the low leachability of their heavy metals content. Indeed, the pyrolysis process concentrates heavy metals in SDBs, increasing therefore their immobilization as compared to those contained in sludge incineration residues [9].

The efficiency of SDBs in removing pollutants from aqueous solutions is dependent on their physico-chemical properties such as the cation exchange capacity, surface area, microporosity, mineral content, and surface functional groups [10]. These properties depend on the raw sludge nature (primary, secondary, activated and digested), pyrolysis and adsorption experimental conditions [11–14]. In order to improve pollutants removal from aqueous solutions using SDBs, different modification methods have been tested as a pretreatment step (on the raw sludge) and/or as a post-treatment stage (on the biochar) [14,15]. These methods are intended to: i) increase the surface area of SDBs, ii) improve their porosity development, and iii) form new and adapted functional groups on their surface.

To date, many review papers have been published on biochar applications for adsorption purposes (145, according to Scopus website retrieved on June 20, 2020 for review papers containing the words “biochar” and “adsorption” in Title, Abstract, Keywords). However, the majority of them deal with lignocellulosic materials. Only 7 review papers have focused on sludge as a feedstock for pyrolysis (according to Scopus website retrieved on June 20, 2020 for review papers containing the words “biochar” and “adsorption” and “sludge” in Title, Abstract, Keywords). Moreover, the attention has mainly been paid on SDBs production, characterization and applications in agriculture [3], construction [6], and for the removal of specific pollutants from wastewaters [13]. Recently, Liu et al. [10] published an excellent review on the SDBs’ characteristics compared to other biochars followed by their reuse as: (i) efficient adsorbents for wastewater treatment, (ii) eco-friendly fertilizers in agriculture with a focus on their possible toxicity, (iii) catalysts for thermochemical conversion, and (iv) carbonaceous materials for energy recovery. The current review provides an in-depth evaluation of the influence of SDBs synthesis conditions on their efficiency in removing both inorganic and organic pollutants from wastewaters. Moreover, a critical evaluation of the underlying adsorption mechanisms is an important contribution of this review. The application of such cost-effective adsorbents for wastewater treatment permits to substantially reduce the use of expensive activated carbon as well as the environment protection against pollution risks generated by the current used raw sludge management options. Therefore, this review aims to summarize and critically analyze the existing studies related to the impact of raw sludge type and pyrolysis conditions on SDBs physico-chemical properties. A special attention was paid to the role of modification methods on both the improvement of SDBs properties and contaminants removal capacities as well as the involved mechanisms.

2. Production and properties of sludge-derived biochars

2.1. Raw sludge production, properties and management policy

Wastewater generation is continuously increasing with the growing

world population and the diversification of industrial activities. These wastewaters, if released raw into the ecosystem, can affect the biota and degrade natural resources [16]. Therefore, wastewater treatment is fundamental to preserve the environment by eliminating hazardous materials before discharge and/or reuse [4,17]. Unfortunately, the treatment processes could generate residual solid byproducts called sludge. The huge generated amounts of sludge have been considered for a longtime as wastes since they could pose serious management challenges due to their origin and complex composition. Indeed, sludge volume and composition vary largely with the geographic area, local conditions, onsite treatment operations (stabilization, conditioning, thickening, digestion, etc.), wastewater nature (urban, industrial, etc.), and even seasonally within the same WWTP [18]. In most cases, freshly generated sewage sludge is initially characterized for its specific gravity, dry matter content, and sludge volume index. The pH of sewage sludge is normally within a neutral range (7.0–8.5). Generally, it contains about 20% of lipids, 50% of carbohydrates (sugar, starch, and fiber), 17%–23% of organic carbon, 3% of total nitrogen, 1.5% of total phosphorus, 0.7% of potassium and a C:N ratio comprised between 10 and 20 [19]. In addition to beneficial components such as organic carbon and macro- and micro-nutrients, hazardous materials are also present in sludge due to their association with the solid phase during wastewater treatment. Their concentrations depend mainly on the raw wastewater origin, composition, treatment technologies and efficiency. Heavy metals or potential toxic elements (PTEs) are the most explored pollutants in wastewater and sludge due to their ubiquitous presence, toxicity and low biodegradability [20,21]. Some PTEs are essential trace elements to biota, such as copper (Cu), iron (Fe), nickel (Ni), and zinc (Zn) [22–24]. However, at excessive concentrations, even the essential elements can be toxic like non-beneficial heavy metals, including cadmium (Cd), chromium (Cr), arsenic (As), mercury (Hg), and lead (Pb) [25]. In addition to the inorganic compounds, sludge tends to accumulate organic compounds such as polycyclic aromatic hydrocarbons [26]. Organic pollutants can contaminate the environment and have a negative effect on biota but, in contrast to PTEs, they could be degraded during different phases of sludge pre- or post-treatment [3].

In view of the fact that sludge has a complex composition, including beneficial and hazardous components, its treatment and management represent a growing challenge [3,21]. The sludge treatment cost constitutes approximately half of the wastewater treatment cost. The final sludge composition, stability as well as local management strategies will determine the feasibility of the three most common "color-labelled" management pathways namely, landfilling (black), land application (green), and thermal processes (red). These latter processes mainly include combustion/incineration, gasification, hydrothermal carbonization, and pyrolysis. Among these strategies, pyrolysis, also known as thermolysis, has been racing ahead for sludge management owing to its lower carbon footprint compared to other thermal methods [27]. Moreover, pyrolysis generates: (i) bio-oil that could be reused after an upgrading step [8], (ii) biogas with lower acidic gases and dioxins contents compared to the incineration process [28], and (iii) biochar that can have various applications in agriculture, environment and energy domains [10].

2.2. Sludge-derived biochars production

The SDBs can be produced, through pyrolysis, in a wide range of installations and reactors, operating under different conditions (heating rate, final temperature, residence time, particle size, etc.). It leads to a very large variety of biochars with different characteristics in terms of structure, morphology, composition, etc. This technique allows long vapor residence time within the solid particle and therefore more efficient secondary cracking reactions [29]. Such conditions are ensured by pyrolysis (conventional or microwave-assisted), torrefaction or/and gasification (Table 1). Recently, hydrothermal carbonization has started gaining ground [30,31]. Its principle is the treatment of the wet sludge with hot compressed water, avoiding the costly drying step (Table 1). Again, here, our interest will be centered on the properties controlling the SDBs applications for wastewater treatment through adsorption.

It is important to underline that the pyrolysis process permits the decomposition of organic materials at temperatures above 350 °C under anoxic conditions [45]. It can be categorized as slow and fast pyrolysis. Fast pyrolysis converts biomass at rapid heating rates, which maximizes the liquid and gaseous fractions [46]. In contrast, slow pyrolysis, operates at long residence times and slow heating rates, maximizing the solid fraction (biochar). At industrial level, slow pyrolysis is carried out with low energy requirements, easier by-products separation and heat recovery possibilities [34]. This thermochemical process is often preceded by a pretreatment procedure of the raw sludge to ensure a proper progress of the operation. It includes all or some of the following steps: dewatering (removal of water), drying (removal of moisture and other liquids than water), and pelletizing for easier handling and transport by mixing with additives (admixtures).

2.3. Sludge-derived biochars characterization

The physical, chemical, textural, and morphological properties of SDBs affect significantly its final usage. Therefore, its thorough characterization before application is essential and for that, more or less sophisticated analytical apparatus such as SEM/EDS, FTIR, MNR, Raman, XPS, XRD etc. are often used [29]. For wastewater treatment, the required characteristics of SDBs include a large specific surface area, a developed pore network dominated by micropores, an enriched surface functional groups, a higher polarity, and the presence of some specific mineral components such as Fe, Ca and Mg [47]. Generally, SDBs have lower carbon (C) content compared to lignocellulosic biomass-derived biochars (Table S1) (15–50% versus up to 95%) [32,48–50]. Consequently, its molar H/C ratio is relatively higher (Table S1 and Fig. 1), especially at high pyrolytic temperatures, where 0.7 to 0.9 ratios are common [35,41,51,52]. This ratio indicates the degree of carbon stability and the proportion of fused aromatic ring structures. The lower is the ratio, the greater is the stability and the more converted is the material. These low ratios are generally reached for slow heating rates [53,54].

In general, high ash content of biochar is advantageous for adsorption applications [55]. Indeed, the minerals left in the pores after the thermal process might contribute to enhance adsorption by different mechanisms. SDBs are often rich in minerals (~65%) (Table S1 and Fig. 1) [33,52,56]. Contrarily to potassium and sodium, low amounts of nitrogen are found in sludge biochars, as nitrogen-containing

Table 1
Processes of biochar production from sludge (* under pressure).

Parameter	Slow Pyrolysis	Fast Pyrolysis	Flash Pyrolysis*	Torrefaction	Gasification	Hydrothermal carbonization
Temperature (°C)	>400	300–1200	800–1300	200–400	500–1300	150–300
Heating rate (°C/s)	<1	10–300	>1000	<1	–	–
Residence time	5 min - 12 h	<5 s	<1 s	30 min–4 h	<1 min	5 min–4 h
Biochar yield (% wt)	15–35	10–30	15–25	5–15	5–15	5–45
Reference	[32–34]	[35,36]	[37,38]	[39,40]	[41,42]	[30,43,44]

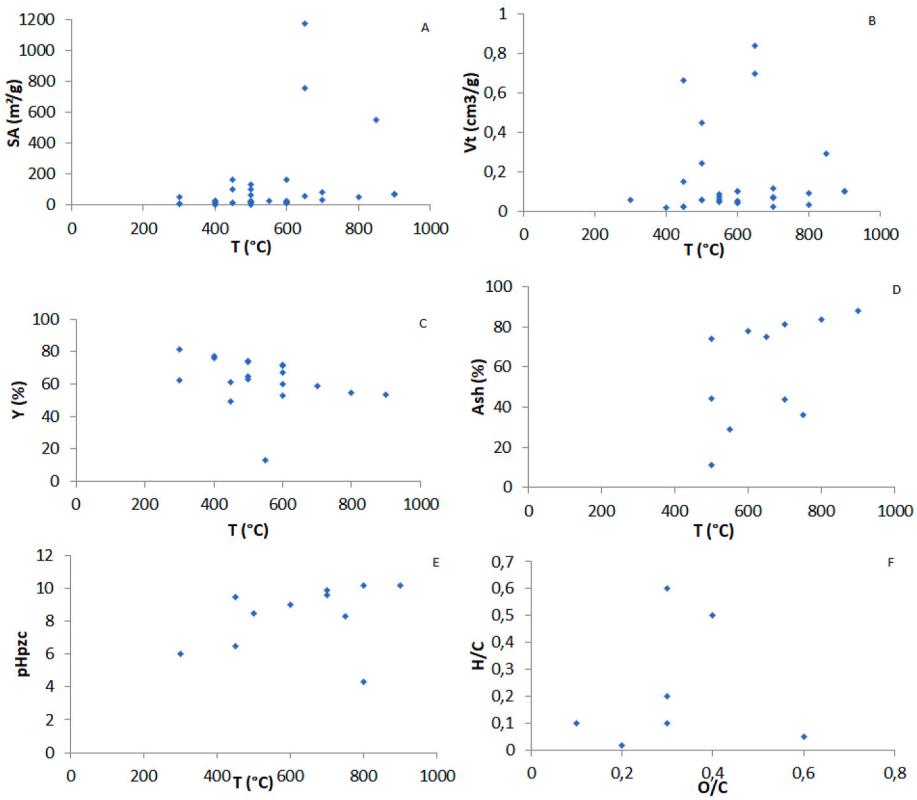

Fig. 1. Effect of pyrolysis temperature on main SDBs properties: (A) specific area (SA), (B) total pore volume (Vt), (C) biochar yield (Y), (D) ash content, (E) pH of zero-point-charge (pHpzc) and (F) Van Krevelen diagram H/C = f (O/C).

compounds are generally decomposed during the charring process (0.2% for high final temperature to 7% at low to moderate ones) [52,57]. SDBs contain also cationic metals (Ca, Mg, Fe, Na, etc.), which play a non-negligible role in adsorption by providing binding sites to negatively charged ions in liquid effluents [58]. Indeed, the sorption process may involve electrostatic interactions between the pollutant molecules and some active sites in biochars. Moreover, its pH and point of zero charge (PZC), which contributes to measuring the surface charge distribution of porous carbons, are important during liquid effluent treatment (Table S1 and Fig. 1). On the contrary, the presence of heavy metals such as Cd, Cu, Zn, Ni, etc., in biochars could hinder their application in adsorption processes [59]. Moreover, heavy metals contained in the raw sludge, are concentrated in the residual fraction of the SDBs making them less mobile than those contained in sludge-incineration residues [60].

The surface chemistry of SDBs is related to the presence of certain chemical elements. Heteroatoms such as hydrogen, oxygen, sulfur and nitrogen might be involved in surface complex functionalities that may be acid (anhydrides, carboxyles, lactols, phenols, lactones, etc.), basic (quinone, pyrone, chromene, nitrogen groups, etc.), or neutral (ethers, carbonyls, etc.) [61]. Alkali metals, mainly sodium and potassium, and alkaline earth metals, such as calcium and magnesium, in the form of carbonates give also a basic feature to SDBs [57]. Moreover, textural properties (specific surface area, micropore volume, etc.) are crucial when dealing with surface mechanisms related sorption, while the pore size and interconnection are implied during the inner migration of the adsorbed molecules [62,63]. For sludge biochars, surface areas of 10–150 m^2/g [33,64,65] and pore volumes (up to 0.1 cm^3/g) [52] are in the same range as other biomass-derived chars [29,66]. The porosity of the SDBs is increased in comparison with the raw sludge due to the volatile matter release. The water released by the dehydroxylation of inorganic material helps also (micro)pore formation [67]. This is important, as micropores development is more favorable than other pores in preparing an adsorbent. Nevertheless, most SDBs are reported to be mesoporous [68]. The best adsorptive biochar performances have been almost correlated to microporous structure, revealed by isotherms of nitrogen adsorption for various SDBs [59,68].

After activation, the specific surface area of SDBs can attain values around 1000 $m^2\ g^{-1}$, which is lower than some commercial activated carbons (1000–2000 $m^2\ g^{-1}$). However, their adsorption capacity may be more effective than some activated carbons in removing specific contaminants such as H_2S and NO_x generated during the thermochemical processes [69,70]. These biochars have also found to efficiently adsorbing metals, phenols and dyes [47,71].

2.4. Impact of experimental conditions on sludge-derived biochars properties

The entire charring process, as well as the pre and the post-treatment procedures influence SDBs properties. It is well known that biochar yield is higher at low temperatures but, in general, the properties required in SDBs as adsorbent are obtained at high temperatures and with additional activation processes [29]. Generally, 600 °C is the temperature required to completely remove the volatile matter from sludge, yielding chars suitable to be activated carbons [29]. When the temperature rises during pyrolysis, C, H, N, S, and H/C ratio decrease (Table S1), while heavy metals concentrations increase [43,58]. Heavy metals contents per dry matter also increases significantly with the pyrolysis residence time [72].

The specific surface areas of SDBs increase with increasing temperature but decrease as the biochar particle size decreases [73]. The second observation may be the consequence of higher ash content in finer grained materials while the first one is attributed to the volatilization of the solid high molecular weight hydrocarbons present on the surface of the biochars [72]. This is the reason why pore structure and surface area development are always correlated, and both are related to the reactor's

temperature and to the residence time [37,53]. As an example, in the work of Lu et al. [74], the micropore structure could not evolve below 650 °C during pyrolysis. At that temperature, mesopores and macropores with an average pore diameter of 120 Å are prevailing, thereby confirming that bubbling causes pore enlargements. At higher temperatures, the biochar acquires more micropores, with an average diameter of 55 Å for 750°C-biochar and 67 Å for 850°C-biochar, but still with less total surface area for the former, which is the consequence of a significant number of mesopores [74]. During pyrolysis, the impact of the residence time on the pore volume distribution has also been investigated. Several authors have reported that the specific surface area, the total pore volume and the average pore width increase significantly with residence time during the thermal treatment by promoting the development of micro- and macro-pores [10,48,67]. In another study, the biochars obtained at 850 °C the mesopores were dominant in 30-min produced chars, and micropores were more numerous for longer residence times during the thermal treatment [53].

On the other hand, pressure may also influence the porosity of biochars. The increase of pressure decreases from slightly to considerably the total surface area, depending on to how much the tar deposits clog the pores [66]. Besides, high pressure brings the aromatic structures to be fused and more extended, with higher carbon content than at atmospheric pressure [38]. It is worth mentioning that an important surface area and a microporous structure do not necessarily confer higher adsorption capacities to the produced biochar. The binding of an adsorbate to a given SDB surface can depend also on the creation of ligand bonds via functional groups. Besides, condensed volatile compounds on the surface and into the biochar's pores during pyrolysis may significantly change the surface functionalization [75].

It is essential to underline that sludge biochars produced at low temperatures are acidic while alkaline at higher ones [10,75]. Most of the active sites are stabilized during pyrolysis and, consequently, the acidic oxygen-containing surface groups are removed from the external carbon surface, making them much fewer than Lewis base sites. Consequently, the pH_{PZC} generally increases [62]. Despite the oxygen-free atmosphere during pyrolysis, oxidation might occur on the external surface when the constituent oxygen of the sludge is liberated, leading to a more uniform surface charge distribution [76].

It is also worth mentioning that sludge pre-treatment may also affect SDB properties in many aspects [5].Because of colloidal materials and polymeric substances found in sludge, coagulation and/or flocculation steps are usually necessary to increase the dewatering efficiency [77].

As the lower is the water content in the sludge cake, the less is the required heat for the primary pyrolysis reactions. Furthermore, the sludge drying temperature set is important as this parameter may influence the release rate of volatiles during the consecutive pyrolysis step and the overall pyrolytic behavior. The impact of this step is also felt on surface area development [78]. On the other hand, post-treatment is usually the step that conditions the biochar to be a potential marketable activated carbon. Physical activation for instance increases the surface area by factors of 10–20 while it is up to 50 fold times with chemical activation (Table S1). Steam activation, as for it, develops uniform pores along with gas formation through on-site surface reaction. It is also noteworthy that washing sludge chars with de-ionized water, acid or base does not necessarily bring significant modifications (Table S1) compared to those given by the nature of the pyrolysis system [75].

3. Use of sludge-derived biochars for wastewater treatment

The sustainable management of the sludge produced worldwide has become an urgent challenge [79]. Instead of landfilling, the application of pyrolysis techniques, allows the production of SDBs with interesting physico-chemical characteristics. The valorization of these SDBs as efficient adsorbents for wastewater treatment in the context of circular economy constitutes a promising and ecofriendly strategy [2].

In general, adsorption studies are performed under static conditions (batch mode) and usually focus on three parts. The first part concerns the physico-chemical characterization of the SDBs (section 2). The second part addresses the adsorptive properties of the used SDBs. It generally includes the assessment of the effects of: i) contact time, ii) adsorbent dosage, iii) pH of the reaction medium, iv) initial pollutant concentration, v) presence of competitive contaminants, and vi) temperature [80]. The experimental kinetic data are commonly confronted to classic models such as pseudo-first-order (PFO) and pseudo-second-order (PSO) models (Table 2). Besides the isothermal data versus temperature are mostly fitted to Langmuir and Freundlich models (Table 2) [81]. These fitting investigations could give qualitative interpretation regarding the possible involved mechanisms as well as the adsorption nature (homogenous/heterogeneous; endothermic/exothermic, spontaneity etc.). The third part concerns the rigorous assessment of the involved mechanisms by interpreting the various physico-chemical analyses of the SDBs before and after the adsorption process [10].

Tables 3 and 4 give a summary of the primary outcomes of various investigations regarding the use of raw and modified SDBs, respectively for the removal of both inorganic (heavy metals and nutrients) and organic pollutants (dyes, pesticides and pharmaceuticals) from aqueous solutions.

3.1. Factors influencing pollutants removal from wastewater by sludge-derived biochars

The efficiency of raw and modified SDBs in removing various chemical compounds (e.g. heavy metals, nutrients, dyes, pharmaceuticals etc.) has been investigated for synthetic and real effluents under static and dynamic conditions [28,70]. It can be clearly deduced that this efficiency is mainly dependent on the physico-chemical properties of SDBs, the contaminant characteristics, and the experimental conditions (Table 3). The major properties of SDBs in this regard include: i) the type and content of surface functional groups, ii) the developed porosity and surface area, and iii) their ion content [44]. These properties could be improved by various thermo-physico-chemical modifications [33,61]. The goal is to produce SDBs with better-developed pore structure and texture including microporous volume abundance, enlarged pore sizes, higher surface area, and denser tailored functional groups (Table 4).

3.1.1. Effect of sludge nature

The used feedstock for biochar production is a key factor that could influence the efficiency of SDBs in pollutants removal. For example, the use of dewatered digested sludge (DDS) instead of dewatered sludge (DS) for the production of SDBs is more beneficial [100]. Accordingly, DDS biochar exhibits better porosity and higher specific surface area for a an improved Pb(II) and P removal efficiency from aqueous solutions. For instance, the SDB generated from a digested dairy waste presented a surface area (161.2 $m^2\ g^{-1}$) and relatively important lead (Pb(II)) removal capacity (51.4 mg g^{-1}) [100]. This high Pb(II) removal capacity

Table 2
Most used kinetic and equilibrium models' original and linearized equations for the fitting of experimental data.

Name	Original equation	Linearized equation
Kinetic model		
Pseudo first-order model (PFO)	$q_t = q_e[Exp(lnq_e - k_1 t)]$	$Ln(q_e - q_t) = \mathrm{Ln}(q_{e,I}) - k_1 t$
Pseudo second-order (PSO)	$q_t = \frac{q_e^2 k_2 t}{q_e k_2 t + 1}$	$\frac{t}{q_t} = \frac{1}{k_2\, q_{e,II}^2} + \frac{1}{q_{e,II}} t$
Equilibrium model		
Langmuir	$q_e = \frac{q_{max} \cdot K_L \cdot C_e}{1 + K_L \cdot C_e}$	$\frac{C_e}{q_e} = \frac{1}{K_L \cdot q_{max}} + \frac{1}{q_{max}} C_e$
Freundlich	$q_e = K_F \cdot C_e^{1/n_F}$	$Ln(q_e) = Ln(K_F) \cdot \frac{1}{\mathrm{n}} + Ln\,(C_e)$

Table 3
Effect of sludge nature and pyrolysis conditions on removing of mineral and organic compounds from aqueous solutions (T = final pyrolysis temperature; G = pyrolysis gradient temperature; t = residence time; qmax: pollutant adsorption capacity; PFO: pseudo-first-order; PSO: pseudo-second order; Lang.: Langmuir; Freun.: Freundlich).

Sludge provenance	Pre-treatment	Pyrolysis conditions	Post-treatment	Adsorption conditions	Pollutant	Kinetic model	Isotherm	qmax (mg/g)	Dominated sorption mechanism	Ref.
Minerals										
Anaerobically digested sludge from a municipal WWTP in Harbin, China	–	T = 600 °C G = 15 °C/min t = 1.5 h	–	C = 200 mg/L D = 1 g/L pH = 6 t = 24 h T = 20 °C	Pb(II)	PSO	Lang.	49.9	Electrostatic attraction, Precipitation, Complexation, Ion exchange	[81]
Anaerobically (primary and secondary) digested sludge, China	–	T = 600 °C t = 2 h	–	C = 0.1–1 mmol/L D = 0.5 g/L pH = 7 t = 12 h T = 22 °C	Pb(II) Cd(II)	–	Lang.	126.4 49.5	Complexation	[82]
Sludge from an industrial WWTP, Belgium	–	Slow pyrolysis: T = 450 °C G = 5 °C/min t = 1.5 h	Washing with HCl solutions and distilled water	C = 2–50 mg/L D = 0.6 g/L pH = 5 t = 48 h	Cu(II) Zn(II)	PSO	Lang. Freun.	3.9 9.1	Cation exchange (dominant) Precipitation Complexation	[83]
		Fast pyrolysis: T = 450 °C		T = 20 °C	Cu(II) Zn(II)			25.7 44.2		
85% of Sludge from an industrial WWTP and 15% of a filter cake, Belgium	–	Slow pyrolysis: T = 450 °C G = 5 °C/min t = 1.5 h			Cu(II) Zn(II)			41.7 38.2		
		Fast pyrolysis: T = 450 °C			Cu(II) Zn(II)			21.8 69.0		
Sludge from a WWTP in Beijing, China,	–	T = 900 °C fast pyrolysis t = 20 min	–	C = 200 mg/L D = 2 g/L pH = 5.7 t = 24 h T = 25 °C	Cr(III) Cr(VI)	– –	– –	22.3 6.5	Surface precipitation and cation exchange	[84]
				C = 200 mg/L D = 2 g/L pH = 4 t = 24 h T = 25 °C	Cd(II)	–	–	42.8	Precipitation and cation exchange	[85]
	–	T = 500 °C fast pyrolysis t = 20 min		C = 50 mg/L D = 2 g/L pH = not adjusted t = 4 h T = 25 °C	Cd(II)	–	–	5.0	Precipitation and cation exchange	[86]
Sludge from a municipal WWTP in Guangzhou, China	–	T = 300 °C G = 20 °C/min t = 2 h	–	C = 5–200 mg/L D = 2 g/L pH = 5 t = 24 h T = 25 °C	Pb(II)	PSO	Lang.	12.6	Cationic exchange Complexation Precipitation	[36]
		T = 400 °C G = 20 °C/min t = 1 h						15.3		
		T = 400 °C G = 20 °C/min t = 2 h						18.2		
		T = 500 °C G = 20 °C/min t = 1 h						16.6		
		T = 500 °C G = 20 °C/min t = 2 h						15.4		
		T = 600-°C G = 20 °C/min t = 1 h						12.4		
		T = 600-°C G = 20 °C/min t = 2 h						12.8		
Sludge from a WWTP in Guangzhou, Guangdong, China	–	T = 600 °C G = 10 °C/min t = 3 h	–	C(Pb) = 30 mg/L C(Cr) = 15 mg/L	Cr(VI) Pb(II)	PSO	–	3.4 2.3	Precipitation Complexation Cation exchange	[87]
			–			PFO	–			

(*continued on next page*)

Table 3 (*continued*)

Sludge provenance	Pre-treatment	Pyrolysis conditions	Post-treatment	Adsorption conditions	Pollutant	Kinetic model	Isotherm	qmax (mg/g)	Dominated sorption mechanism	Ref.
	Mixture with Starch at a dose of 50:2 (sludge/starch)			D = 1.5 g/L pH = 4 t = 30 min	Cr(VI) Pb(II)			19.8 9.1	Precipitation Complexation Cation exchange Reduction	
Sludge from a municipal WWTP in Guangzhou, China	–	T = 400 °C G = 20 °C/min t = 2 h	–	D = 1 g/L pH = 5 t = 24 h T = 25 °C	Pb(II) Cr(VI)	PSO PSO	Lang. Lang.	40.8 24.4	Complexation Precipitation Reduction, complexation and precipitation	[88]
				C = 0.1–30 mg/L D = 2 g/L pH = 6 t = 24 h T = 25 °C	As(III)	PSO	Freun.	6.04	Ligand exchange with hydroxyl groups	[89]
Sludge from the municipal WWTP, Chania, Greece	–	T = 300 °C G = 17 °C/min t = 1 h	–	C = 90–850 mg/L D = 4 g/L pH = 6.7–7 t = 24 h, Ambient T	As(V) Cr(III) Cr(VI)	PSO	Freun.	13.4 94.3 64.1	Electrostatic attraction precipitation	[90]
Sludge from urban WWTP, Guangdong, China	–	T = 500 °C G = 5 °C/min t = 4 h	–	C = 20–200 mg/L D = 1 g/L pH = 3 t = 20 h T = 25 °C	Cu(II)	–	Lang.	3.2	Complexation Cation exchange Electrostatic attraction	[91]
Dewatered sludge from urban WWTP Qinhuangdao, China	Mixing with dolomite at a ratio of 1:1 (Mass)	T = 800 °C, G = 5 °C/min t = 2 h	–	C = 25–175 mg/L D = 1.2 g/L pH = 4.5 t = 3 h T = 25 °C	P-PO_4	PSO	Lang.	29.2	Electrostatic attraction precipitation	[92]
Sludge from municipal WWTP, Baoding, China	–	T = 300 °C, G = 5 °C/min Then, T = 600 °C G = 10 °C/min t = 2 h	–	C = 50 mg/L D = 2 g/L t = 36 h Ambient T	NH_4 PO_4	– PSO	–	0.6 50.0	For NH_4, mainly complexation For P, mainly electrostatic attraction, complexation, precipitation	[93]
	Mixing with walnut shell at a ratio of 3:1 (sludge/walnut shell)				NH_4 PO_4	PSO –		2.3 ~41.5		
	Mixing with walnut shell at a ratio of 1:1				NH_4 PO_4	– –		~1.8 ~38.5		
	Mixing with walnut shell at a ratio of 1:3				NH_4 PO_4	– –		~0.9 ~27.5		
Anaerobically digested sludge from a municipal WWTP, Alberta, Canada	–	T = 450 °C G = 5 °C/min t = 2 h	–	C = 2–80 mg/L D = 10 g/L t = 24 h T = 20 °C	N–NH_4	PSO	Lang.	1.5	Diffusion Electrostatic attraction Complexation	[94]
Organics										
Mixture of sludge from the WWTP of Wuhan and rice husk biomass (ratio = 1:1)	–	T = 500 °C G = 7 °C/min t = 2 h	–	C = 50–300 mg/L D = 1 g/L pH = 6-7 t = 24 h T = 25 °C	Direct Red 4BS Acid Orange II React Blue 19 Methylene Blue	PSO	Lang.	59.8 38.5 42.1 22.6	Complexation, Electrostatic attraction π-π stacking interaction	[95]
Sludge from urban WWTP, China	–	T = 550 °C G = 10 °C/min t = 2 h	–	C = 50–500 mg/L D = 6 g/L pH = natural, t = 24 h T = 25 °C	Methylene blue	PSO	Lang.	24.1	Electrostatic attraction Cation exchange Complexation n- π conjugate action	[96]
Sludge from municipal WWTP, Bangkok, Thailand	–	T = 350 °C G = 20 °C/min t = 30 min	–	C = 10–750 mg/L D = 3 g/L pH = natural t = 48 h	Acid yellow 49 (AY), Basic blue 41 (BB), Reactive red 198 RR)	–	Lang.	12.7 212.8 12.7	Electrostatic attraction Cationic exchange (BB)	[97]
		T = 450 °C			AY BB RR			26.3 222.2 14.1		

(*continued on next page*)

Table 3 (*continued*)

Sludge provenance	Pre-treatment	Pyrolysis conditions	Post-treatment	Adsorption conditions	Pollutant	Kinetic model	Isotherm	qmax (mg/g)	Dominated sorption mechanism	Ref.
		T = 550 °C			AY			45.4		
					BB			357.1		
					RR			15.2		
		T = 650 °C			AY			65.6		
					BB			384.6		
					RR			17.5		
		T = 750 °C			AY			71.4		
					BB			416.7		
					RR			18.9		
Mixture of paper sludge/wheat husks, Austria	–	T = 500 °C t = 20 min	–	C = 20–60 mg/L D = 4 g/L pH = 2 t = 3 h T = 55 °C	2,4 DCP	PSO	Freun.	17.5	Electrostatic Interactions, pore-filling, hydrophobic forces,	[98]
Sludge from paper mill effluent treatment plant, India	–	T = 600 °C T = 700 °C	–	C = 5–50 mg/L D = 0.5 g/L T = 25 °C	Pentachloro-phenol	–	Lang.	35.9 41.3	Ion exchange Pore filling	[99]

was imputed mainly to the existing mineral contents in the SDBs which contribute to Pb(II) retention by cation exchange process and also precipitation as cerussite ($PbCO_3$), hydrocerussite ($Pb_3(CO_3)_2(OH)_2$), and pyromorphite ($Pb_5(PO_4)_3Cl$). Ho et al. [81] studied the feedstock role in removing six individual heavy metals. These authors produced six biochars derived from waste-activated-sludge (WAS) and anaerobically-digested-sludge (ADS) using pyrolysis process at 400, 600 and 800 °C. They found that the highest removal capacities of Pb(II), Cd (II), Cu(II), Zn(II), Ni(II), and Cr(VI) correspond to the biochar of ADS generated at 600 °C. These findings were attributed to the higher pH value and mineral contents especially Al, Ca, Fe, K, Mg, and P of the ADS. In particular, it was proved that more than 86% of Pb(II) removal occurs through metal ion exchange and precipitation with minerals [81]. Agrafioti et al. [90] confirmed these findings when a SDB rich in CaO (17.4%), Fe_2O_3 (12.5%), and Al_2O_3 (5.3%) was used for Cr(III) and Cr(VI) removal [90]. Accordingly, this SDB successfully removed about 94.3 mg g^{-1} of Cr(III) and 64.1 mg g^{-1} of Cr(VI), which are about 4.2 and 9.9 times higher than the ones reported for another SDB having lower mineral contents [86] (Table 3). Moreover, Kalderis et al. [98] showed that higher Ca and K contents in SDBs from the pyrolysis of a mixture of sludge and wheat husks could promote 2,4 DCP adsorption [98].

On the other hand, the pyrolysis of aerobic (A) and anaerobic sludge (AN) under the same experimental conditions resulted in AN-SDBs with better physico-chemical properties compared to A-SDBs [101]. Under the same experimental conditions (initial Fe(III) concentration of 100 mg/L; adsorbent dosage of 5 g/L and a pH of 2), Fe(III) removal efficiency was evaluated to 99.7% and 65.0% for the AN-SDBs and A-SDBs, respectively. Since the measured surface areas and micropore volumes were quite similar for both biochars (105 m^2 g^{-1} and 0.04 cm^3 g^{-1}, and 102 m^2 g^{-1} and 0.04 cm^3 g^{-1} for AN-SDBs and A-SDBs, respectively), these findings were linked to the existence of more functional groups at the surface of the AN-SDBs such as carboxylic acids and anhydrides, lactones, phenols, ethers, and quinines.

For specific pollutants, such as N–NH_4, it has been recommended to mix the sludge with lignocellulosic biomass (such as walnut shells (WS)) before their co-pyrolysis in order to produce SDBs with more developed porosity and higher surface area. In this context, Yin et al. [93] studied N–NH_4 and P-PO_4 removal from aqueous solutions by SDB generated from the slow pyrolysis of different ratios of mixed municipal sludge/WS (1:0; 3:1; 1:1 and 1:3) at 600 °C. The biochar surface area and micropore volume increased with the lignocellulosic fraction increase from 31.35 m^2 g^{-1} and 0.0034 cm^3 g^{-1} (raw sludge only) to 122.89 m^2 g^{-1} and 0.0297 cm^3 g^{-1} for a sludge/WS ratio of 1:3. Consequently, they reported an increase of N–NH_4 adsorption from 0.62 mg g^{-1} for the raw SDB to 2.31 mg g^{-1} for the one derived from the co-pyrolysis of mixed sludge with WS at a ratio of 1:3 (Table 3). Contrary to N–NH_4, the adsorption efficiency of P-PO_4 increased with an increase in the sludge proportion. The highest adsorption capacity (49.95 mg g^{-1}) was observed for the biochar derived from the raw sludge. Since this biochar had the lowest surface area, they concluded that this parameter was not the major factor influencing P-PO_4 adsorption. They attributed this behavior to the SDB richness in several metal elements (especially Ca, Mg, Al, and Fe) and various surface functional groups (mainly Si–O, Mg–O, and Al–O bonds) [93]. In the same context, Nielsen et al. [102] showed that the mix of raw anaerobic digested sludge with fish wastes at a ratio of 9:1 and their pyrolysis at 950 °C doubled the adsorption capacity of carbamazepine (toxic pharmaceutical product). This behavior was attributed to the fact that fish wastes favor the presence of highly dispersed polar inorganic phase and carbon, providing more hydrophobicity in micropores [102].

3.1.2. *Effect of pyrolysis conditions*

The adsorption capacity of SDBs depends on pyrolysis conditions. It appears that compared to fast pyrolysis, slow pyrolysis induces the encapsulation of various exchangeable cations limiting their exchange with heavy metals contained in effluents [83]. Even if the SDBs produced by slow or fast pyrolysis have relatively similar mineral contents, the cation exchange process between the Ca(II), Mg(II) and K(I) existing in the SDB from slow pyrolysis and Cu(II) and Zn(II) contained in synthetic solutions is very much limited [83]. For that reason, the adsorption capacities of Cu(II) and Zn(II) by the SDBs generated from the fast pyrolysis were assessed to 25.7 and 44.2 mg g^{-1} which are about 2.3 and 1.7 times higher than the ones related to slow pyrolysis [83]. On the other hand, the use of the electromagnetic induction method (EMI), as a new, efficient, fast, and energy-saving heating method, for the production of SDBs seems to significantly impact the nature and contents of the formed functional groups [103]. Accordingly, the SDBs produced at 500 °C, even if they have very low specific surface area and micropore volume (2.8 m^2 g^{-1} and 0.0014 cm^3 g^{-1}, respectively), successfully removed 198.1 and 178.0 mg g^{-1} of Pb(II) and Cd(II), respectively (Table 4). These spectacular removal capacities were attributed to the formation of abundant functional groups (due to EMI treatment) such as hydroxyl, aliphatic, amide, aromatic, and hetero-aromatic groups etc., that efficiently react with these two toxic metals. Furthermore, the aromatic carbon in the produced SDBs through the conversion of alkyl and O alkyl to aryl C provided π electron, which can efficiently bond with heavy metal cations.

Table 4
Effect of sludge modification on removing mineral and organic compounds from aqueous solutions (T = final pyrolysis temperature; G = pyrolysis gradient temperature; t = residence time; qmax: pollutant adsorption capacity; PFO: pseudo-first-order; PSO: pseudo-second-order; Lang.: Langmuir; Freun.: Freundlich).

Sludge, provenance	Pre-treatment	Pyrolysis conditions	Post-treatment	Adsorption conditions	Pollutant	Kinetic model	Isotherm	qmax (mg/g)	Dominated sorption mechanisms	Ref.
Minerals										
Aerobic Sludge from WWTP, region of Madrid, Spain	–	T = 450 °C G = 10 °C/min t = 1 h	Physical activation with air for 4 h at 275 °C	C = 100 mg/L D = 5 g/L pH = 2 t = 1 h	Fe(III)	–	–	13.0	–	[101]
Anaerobic Sludge from WWTP, region of Madrid, Spain								19.9		
Sludge from WWTP in Wuhan, China	–	T = 700 °C G = 10 °C/min t = 1 h	– Physical activation with CO_2 at 700 °C for 1 h Chemical activation with KOH: Ratio biochar/KOH = 1:2, then heating at 700 °C for 1 h Chemical activation with CH_3COOK: Ratio biochar/CH_3COOH = 1:2 then heating at 700 °C for 1 h	C = 5–300 mg/L D = 2 g/L pH = 7 t = 24 h T = 22 °C	Pb(II)	PSO PSO PSO PFO	Lang.	7.6 22.4 57.5 47.6	Electrostatic attraction Precipitation Complexation	[119]
Sludge from a WWTP of a dairy industry, Amol, Iran	Impregnation of sludge in 5 M $ZnCl_2$ solution. Mass ratio Sludge/$ZnCl_2$ solution = 1:3)	T = 650 °C G = 10 °C/min t = 1 h	–	C = 50–250 mg/L D = 3 g/L pH = 2 t = 2 h T = 25 °C	Cr(VI)	PSO	Freun.	72.8	–	[110]
Anaerobically digested sludge from a WWTP in Portugal	–	T = 650 °C G = 40 °C/min t = 30 min	–	C = 10–2000 mg/L D = 10 g/L pH = 5 t = 24 h T = 25 °C	Hg(II) Pb(II) Cu(II) Cr(III)	–	Lang.	62.6 27.4 3.6 5.6	–	[114]
	Impregnation in $ZnCl_2$. Mass ratio = 1:1				Hg(II) Pb(II) Cu(II) Cr(III)			137.2 33.0 16.5 2.2		
Sludge from a municipal WWTP, Changsha, china	Impregnation with $ZnCl_2$ solution	T = 850 °C G = – t = –	washing with HCl solution	C = 5–80 mg/L D = 5 g/L pH = 5.8 t = 3 h T = room temperature	Cd(II) Ni(II)	–	Lang.	16.7 9.1	Ion exchange	[116]
Aerobic granular sludge from a lab-scale SBR	Impregnation of 10 g of sludge in 25 mL of a $ZnCl_2$ solution (5 M)	T = 600 °C G = – t = 2 h	Washing with 3 M HCl solution	C = 5–80 mg/L D = 1 g/L pH = 5 t = 48 h T = 25 °C	Cu(II)	PSO	Freun.	18.5	Precipitation Complexation Cation exchange	[115]
Sludge from a municipal WWTP in Tianjin, China		Heating/pyrolysis with a microwave (9.6 kW) T = 700 °C G = 6.5 °C/min t = 20 min	–	C = 10–160 mg/L D = 2 g/L pH = 5 t = 1 h T = 20 °C	Pb(II) Cu(II)		Lang.	41.0 31.7	Complexation Precipitation Cation exchange	[106]
	Impregnation with KOH solution. Mass ratio sludge/KOH = 1:0.1	Heating/pyrolysis with a microwave (8 kW) T = 600 °C G = 6.5 °C/min t = 20 min	Washing with 3 M HCl		Pb(II) Cu(II)			49.7 42.0		
	Impregnation with H_3PO_4 solution				Pb(II) Cu(II)			55.9 46.3		
	Impregnation with $ZnCl_2$				Pb(II) Cu(II)			47.4 37.4		

(*continued on next page*)

Table 4 (*continued*)

Sludge, provenance	Pre-treatment	Pyrolysis conditions	Post-treatment	Adsorption conditions	Pollutant	Kinetic model	Isotherm	qmax (mg/g)	Dominated sorption mechanisms	Ref.
	solution. Mass ratio sludge/ $ZnCl_2$ = 1:0.15									
Sludge from textile Treatment Plant in Denizli, Turkey	Impregnation with KOH. Mass ratio = 1:1	T = 500 °C G = – t = 1 h	Washing with HCl solutions and drying	C = 10–90 mg/L D = 6.67 g/L pH = 6 t = 1 h T = 40 °C	Sr(II)	–	Freun.	138.9	Ion exchange	[113]
Sludge from a municipal WWTP in Madrid, Spain	–	T = 450 °C G = 3 °C/min t = 1 h	–	C Na(I) = 10,500 mg/L C K(I) = 380 mg/L C Ca(II) = 450 mg/L C Mg(II) = 1350 mg/L D = 5 g/L pH = – t = 3 h T = –	Na(I) K(I) Ca(II) Mg(II)	–		1612.4 50.2 28.1 115.7	Cation exchange Complexation	[107]
	Impregnation in H_2SO_4 solution. Ratio Sludge/ H2SO4 = 1:1 (M/V)				Na(I) K(I) Ca(II) Mg(II)			1462.9 43.9 9.9 121.1		
Sludge from a municipal WWTP, china	Impregnation with H2SO4 solution 40%. Ratio sludge/ solution = 1:1 (M/V)	T = 500 °C G = – t = 30 min	–	C = 25–240 mg/L D = 1.4 g/L pH = 1 t = 10 h T = 25 °C	Cr(VI)	PSO	Lang.	59.5	Electrostatic attraction Complexation	[109]
Sludge from Taiping municipal WWTP in Harbin, China	–	T = 600 °C G = 15 °C/min t = 90 min	–	C = 100 mg/L D = 1 g/L t = 8 h T = ambient	Cd(II) Pb(II) Cu(II) Ni(II) Zn(II)	–	–	~15 ~31 ~8 ~14 ~9		[59]
	Pretreatment with persulfate-Zero-Valent Iron		–		Cd(II) Pb(II) Cu(II) Ni(II) Zn(II)	PSO	–	33.9 50.0 36.8 29.5 30.1	Electrostatic attraction Ion exchange Pollutant Reduction by the nZVI Complexation	
Dewatered sludge from a Municipal WWTP in Wuhan, China	–	T = 400 °C G = – t = 2 h	Coating of Carboxymethyl Chitosan onto the produced biochar	C = 20–1500 mg/L D = 0.6 g/L, pH = 3 (Hg (II)) pH = 5 (Pb(II)) t = 24 h T = 30 °C	Hg(II) Pb(II)	PSO PSO	Lang.	769.2 239.2	Complexation	[121]
Sludge from urban WWTP, Beijing, China	–	T = 500 °C G = – t = 1 h	– Amino-functionalization	C = 10–2000 mg/L D = 1 g/L pH = 5.5 t = 24 h T = 30 °C	Cu(II)	PSO	Sips	34.2 74.5	Complexation with –OH Complexation with -NH2	[122]
Dewatered Sludge from a municipal WWTP, Wuhan, china	–	Electromagnetic induction T = 500 °C t = 30 min	–	C = 10–320 mg/L D = 5 g/L pH = 7 t = 6 h T = 20 °C	Pb(II) Cd(II)	PFO	Lang.	198.1 178.0	Complexation	[103]
Sludge from urban WWTP, Wisconsin, USA	–	T = 450 °C G = – t = 1.5 h	Activation with KOH 2 N	C = 650 mg/L D = 10 g/L pH = – t = 24 h T = –	$N–NH_4$	–	–	5.3	–	[123]
Anaerobically digested sludge from WWTP, England	–	T = 550 °C G = – t = – T = 700 °C G = – t = –	– Activation with CO_2 at 800C –	C = 50 mg/L D = 50 g/L pH = – t = 48 h T = 25 °C	$P-PO_4$	–	–	0.7 1.2 0.5	Electrostatic attraction Complexation precipitation	[104]

(*continued on next page*)

Table 4 (*continued*)

Sludge, provenance	Pre-treatment	Pyrolysis conditions	Post-treatment	Adsorption conditions	Pollutant	Kinetic model	Isotherm	qmax (mg/g)	Dominated sorption mechanisms	Ref.
Anaerobically digested sludge from a municipal WWTP, Iran	Impregnation with $CaCl_2$ solutions	T = 700 °C G = – t = 3 h	–	C = 30–600 mg/L D = 2 g/L pH = 7 t = 24 h T = 25 °C	P-PO_4	PSO	Lang.	153.9	Diffusion Complexation	[105]
Organics										
Primary sludge from a paper mill industry, Portugal	–	T = 800 °C G = 10 °C/min t = 10 min	–	C = 10–20 mg/L D = 0.075 for raw, KOH and NaOH biochars and 0.2 g/L for $ZnCl_2$ biochar t = 8 h T = 25 °C	Fluoxetine-HCl	PSO	Zhu-Gu	120.4	electrostatic interactions	[124]
	Impregnation with KOH. Mass ratio = 1:1						Zhu-Gu	191.6	π-π interaction	
	Impregnation with NaOH. Mass ratio = 1:1						Zhu-Gu	136.6	π-π interaction	
	Impregnation with $ZnCl_2$. Mass ratio = 1:1						Sips	29.6	electrostatic interactions	
Dewatered sludge from a WWTP of a petrochemical industry, Taiwan	Impregnation in $ZnCl_2$ solution (1 M)	T = 500 °C G = 15 °C/min t = 30 min	Washing with HCl solution (3 N)	C = 30–80 mg/L D = 0.05 g/L pH = 7 t = 20 days T = 30 °C	Orange II Chrysophenine	–	Lang.	350.0 190.0	–	[120]
Dewatered sludge from WWTP in Guangzhou, China	Impregnation of 40 g of sludge in 100 mL of citric acid (2 M) and $ZnCl_2$ (0.5 M)	T = 500 °C G = 20 °C/min t = 1 h	Washing with HCl solution	C = 0.5–50 mmol/L D = 1 g/L pH = 4 t = 6 h T = 25 °C	4-Hydroxybenzoic acid phenol, benzoic acid, 4-chlorophenol		Lang.	258.0 130.6 266.8 256.2	pore-filling, hydrophobic interactions	[125]
Aerobic granular sludge from a lab-scale SBR	Impregnation of 10 g of sludge in 25 mL of $ZnCl_2$ solution (5 M)	T = 650 °C G = 5 °C/min t = 2 h	Washing with 3 M HCl solution	C = 20–500 mg/L D = 0.5 g/L pH = 6 t = 5 h T = 25 °C	Methylene blue	PSO	Lang.	323.7	Complexation	[11]
Aerobic sludge from a municipal WWTP in Jinan, China								144.8		
Biochemical sludge from a WWTP, China	Activation for 2 h with a mixture of 5 M $ZnCl_2$ and 5 M H_2SO_4 with a ratio $ZnCl/H_2SO_4$ = 1:2 (V/V). Ratio Solid/liquid = 1:2.5 (M/V)	T = 550 °C G = 5 °C/min t = 2 h	Washing with 3 M HCl solution	Real wastewater. COD = 302.4 mg/L P-PO_4 = 19.7 mg/L D = 5 g/L pH = 8.5 t = 10 min T = ambient	Organics P-PO_4	–	–	47.8 3.9	–	[40]
Surplus sludge from a WWTP, China					Organics P-PO_4			41.3 3.8		
Biochemical sludge from a petrochemistry company					Organics P-PO_4			45.7 3.9		
Sludge from a WWTP, Grenada, Spain	–	T = 700 °C G = 10 °C/min t = 3 h	—	t = 8 days T = 25 °C	Tetracycline 2,4 DCP MB Cd	–	Lang.	366.7 29.3 204.7 32.6	π-π interaction Electrostatic attraction Complexation	[39]
	Impregnation of 100 g of sludge with 50 g of NaOH				Tetracycline 2,4 DCP MB Cd(II)			1248.9 55.4 518.2 59.6	Ion exchange (Cd(II))	
	Impregnation of 100 g of sludge with 25 g of NaOH and 20 g of humic acid				Tetracycline 2,4 DCP MB Cd(II)			906.7 26.1 156.8 54.0		
	Impregnation of 100 g of sludge with 25 g of NaOH and 20 g of clay				Tetracycline 2,4 DCP MB Cd(II)			768.9 42.4 262.3 66.3		
	Impregnation of 100 g of				Tetracycline 2,4 DCP			711.1 47.3		

(*continued on next page*)

Table 4 (*continued*)

Sludge, provenance	Pre-treatment	Pyrolysis conditions	Post-treatment	Adsorption conditions	Pollutant	Kinetic model	Isotherm	qmax (mg/g)	Dominated sorption mechanisms	Ref.
	sludge with 25 g of NaOH and 20 g of phenolic resin				MB Cd(II)			483.1 54.0		
Sludge from domestic WWTP in Beijing, China	– pH adjustment to 12 by NaOH (10 M) + thermal treatment at 175 °C for 30 min	T = 600 °C G = – t = 1 h	–	C = 40–400 mg/L D = 1 g/L pH = – t = 24 h T = 25 °C	Cationic red XGRL	PSO	Lang.	42.2 47.1	Electrostatic attraction Chemical adsorption	[126]
Sludge from the urban WWTP in Harbin, China	–	T = 600 °C G = 5 °C/min t = 1 h	– impregnation with NaOH then pyrolysis again at T = 600 °C G = 5 °C/min t = 2 h	C = 10–50 mg/L (RhB) C = 20–150 mg/L (phenol) D = 1 g/L pH = – t = 1 h T = 25 °C	Rhodamine B (RhB) Phenol RhB Phenol	PSO	Lang.	27.7 51.0 35.1 96.2	–	[67]
Sludge from domestic WWTP, Spain	–	T = 625 °C G = 40 °C/min t = 30 min	–	C = 100–1000 mg/L, D = 5 g/L pH = –, t = 25–300 min, T = 25 °C	Crystal violet (CV) Indigo carmine (IC) Phenol (P)	–	Freun.	184.7 30.8 5.6	–	[108]
	Impregnation with H_2SO_4 1:1 (mass ratio)				CV IC P			270.9 54.4 29.5		
Sludge from an industrial WWTP, Mexico	–	T = 500 °C t = 60 min	Impregnation with HCl solution (10%) at 20 °C for 8 h	C = 100–1000 mg/L, D = 10 g/L, pH = 6.5, t = 40 h, T = 30 °C	Indigo Carmin	PFO	Lang.	92.83	Physical adsorption	[127]
Sludge from a paper mill, Taiwan	–	T = 600 °C G = 20 °C/min t = 1 h	Impregnation with 1 M HCl solution	C = 1200–2100 mg/L (MB) C = 500–1200 mg/L (PR), D = 1 g/L, pH = 7.5 (MB) and 3.5 (PR), t = 4 h, T = 30 °C	MB Procion Red MX-5B (PR)	PSO PSO	Lang.	119.0 65.8	π-π interaction Electrostatic attraction	[112]
Sludge from a domestic WWTP, Wuhan, China,	–	T = 800 °C t = 2 h	Magnetization through adding of SrCO3, HCl, $FeCl_3$ and NaOH. Then, pyrolysis at 800C for 2 h	C = 50–700 mg/L, D = 1 g/L, pH = 7, t = 4 h, T = room temperature	Malachite green	PSO	Lang.	404.9	–	[128]
Paper and pulp sludge from a paper mill, Zimbabwe	–	T = 750 °C t = 2 h	–	C = 50–250 mg/L, D = 7.5 g/L, pH = 2, t = 1 h, T = 25 °C	Methyl orange	PSO	Freun.	22.0	Electrostatic attraction Complexation π-π stacking interaction	[117]
	Impregnation with $FeCl_3$ solution 1:3 (M/V)			C = 50–250 mg/L, D = 5 g/L, pH =			Lang.	46.6		

(*continued on next page*)

Table 4 (*continued*)

Sludge, provenance	Pre-treatment	Pyrolysis conditions	Post-treatment	Adsorption conditions	Pollutant	Kinetic model	Isotherm	qmax (mg/g)	Dominated sorption mechanisms	Ref.
sludge from WWTP in Lanzhou, China.	Impregnation of 10 g of sludge in 100 mL $ZnCl_2$ (2 M).	T = 500 °C G = 10 °C/min t = 2 h	Coating with Fe/S nanoparticles	12, t = 1 h, T = 25 °C C = 100–1000 mg/L, D = 2 g/L, pH = 3, t = 4 h, T = 25 °C	Tetracycline	PSO	Lang.	174.1	pore filling, π-π stacking, hydrogen bonding interaction, ion exchange, complexation, electrostatic attraction	[129]
	Impregnation with KOH. Mass ratio sludge/KOH = 2:1		Coating with Fe/Cu nanoparticles	C = 100–1500 mg/L, D = 5 g/L, pH = 4, t = 4 h, T = 25 °C				387.0		[130]

On the other hand, the impact of pyrolysis temperature on the adsorption properties of SDBs has been investigated [14,58,86,89,102]. Generally, the increase in temperature results in a significant increase in carbon content, specific surface areas, porosity (total pore volume, micropore volume, and average pore width), alkalinity, aromaticity, and in the same time in a non-negligible decrease of its polarity, hydrophilicity and surface functional groups due to more losses of O and H compounds [15,33]. The importance of the role played by each parameter cited above depends not only on the raw sludge characteristics and the nature of target pollutants but also on biochar production conditions. In this context, increasing the temperature from 500 to 900 °C for the fast pyrolysis of urban sludge increased the Cd(II) adsorption from about 5.0 to 42.8 mg g^{-1} [85,86]. This was mainly due to the improved physico-chemical properties of the produced biochar at a higher temperature. Indeed, the biochar produced at 900 °C has a specific surface area of 67.6 m^2 g^{-1}, a pore volume of 0.099 cm^3/g and a CEC of 247.51 cmol/kg, which are about 165.9%, 75.7% and 222.5% higher than those measured for the biochar produced at 500 °C. Besides, it appears that the increase of fast pyrolysis temperature transforms the contained minerals into more leachable forms. Indeed, Chen et al. [85,86] showed that for an initial Cd(II) concentration of 175 mg/L in the aqueous solution, the released Ca(II) concentrations were relatively negligible for the biochar produced at 500 °C and more than 55 mg/L for the one produced at 900 °C. Moreover, Nielsen et al. [102] showed that increasing pyrolysis temperature from 650 to 950 °C of a mixture of anaerobically digested sludge/fish wastes at various mass ratios (50:50; 75:25; 90:10) resulted in a better porosity development and a higher surface area. The adsorbed amounts of carbamazepine by the biochars produced at 950 °C are 2–8 times higher than the ones observed for those produced at 650 °C. Finally, the more alkaline biochars produced at higher pyrolysis temperatures led to a greater lead cations precipitation. These combined reasons made the produced SDB at a temperature of 900 °C about ten times more efficient than a commercial activated carbon in removing Cd(II) from aqueous solutions [102]. Similar behavior was reported by Jindarom et al. [97], who showed that the increase of pyrolysis temperature of an urban sludge from 350 to 700 °C increased the adsorption capacities of three dyes by about 462%, 96%, and 49% (Table 3). This behavior was imputed to the increase of the surface area by a factor of more than 2.4. Likewise, when studying triclosan removal by a HCl-pre-treated SDB, Tong et al. [14] found that the related efficiency gradually increased with the increase of pyrolysis temperature from 300 to 800 °C. Moreover, the reported removal efficiency of the biochar produced at 800 °C was even higher than a commercial activated carbon.

It is essential to underline that even if the increase of pyrolysis temperature and residence time improved the SDBs specific surface areas, the removal efficiency of some chemicals was on the contrary decreased as reported for Pb(II) [36], As(III) [89], P-PO_4 [104], and N–NH_4 [94]. This behavior was related to the loss of oxygen-containing surface functional groups and C graphitization due to the deoxygenation and dehydrogenation of sludge with the increase of the pyrolysis temperature. Consequently, for efficient removal of P-PO_4 by SDBs, Melia et al. [104] recommended, for instance, the mixing of the raw sludge with Ca/Mg-rich materials such as dolomite [92] or its impregnation with $CaCl_2$ or $MgCl_2$ solutions [105] instead of increasing pyrolysis temperature [104].

3.1.3. *Effect of modification of raw sludge or its derived biochar*

Various methods have been used for the modification of raw sludge and SDBs in order to improve their texture and surface chemistry for better adsorption capacity. These methods include physical and/or chemical, thermal processes and the SDB-based composites' production through their embedding with different materials [33,70,92].

3.1.3.1. Physico-chemical activation. Physical activation involves steam, CO_2, O_2 or their mixture at relatively high temperatures (usually higher than 700 °C) [33]. Chemical activation involves the impregnation of the raw sludge or the SDBs with various chemical agents such as KOH, NaOH, K_2CO_3, H_3PO_4, H_2SO_4, HCl or $ZnCl_2$ followed by a thermal treatment at moderate temperature (400–500 °C). These methods generally result in the creation of interconnecting micropores network, well-developed surface area, and oxygen-containing functional groups onto which pollutants could be physically and/or chemically adsorbed. The main parameters influencing the characteristics of modified biochars and ultimately their efficiency in removing pollutants are the activating physical/chemical agent's type and dose and the activation temperature [33,35].

Studies related to sludge's physical activation have been carried out by using CO_2 as an activation agent [44,104]. In this context, CO_2 activation was operated for 20 min at 800 °C for biochars prepared from an anaerobically digested sludge pyrolysis at 550 °C [104]. This process increased the surface area and total pore volume by about 5.9 and 1.5 times, respectively, resulting in increased P-PO_4 removal efficiency from 0.74 to 1.15 mg g^{-1}. Besides, Zhang et al. [44] activated SDBs generated at 700 °C using CO_2 at the same temperature and a residence time of 1 h. They showed that compared to the non-activated SDB, the BET surface area of post-activated SDB increased significantly from 81.4 to 239.8 m^2 g^{-1}, and Pb(II) removal capacity by a factor of about 3 (Table 4). However, this Pb(II) removal capacity was lower than that observed after chemical activation by KOH or CH_3COOH, as shown in Table 4 [44]. On the other hand, Méndez et al. [101] investigated the use of physically activated SDBs generated from the pyrolysis of five anaerobic and five aerobic sludge at a temperature of 450 °C for Fe(III) removal from aqueous solutions. They proved that the activation process with air at a temperature of 275 °C for 4 h significantly improved the structure and texture of the biochars generated from both types of sludge. In

particular, the physically activated SDB from the anaerobic sludge had the highest BET surface area (105 $m^2\ g^{-1}$) and micro-porosity (0.04 $cm^3\ g^{-1}$) and permitted a quasi-complete removal of Fe(III) from aqueous solutions for an initial Fe(III) concentration of 100 mg/L, an adsorbent dosage of 5 g/L and a pH of 2 [101].

The chemical activation of SDBs has been carried out with different compounds including acids such as H_3PO_4 [106], H_2SO_4 [107–109], HCl [110–112], alkaline solutions of KOH [113], NaOH [39], and metal salts such as $ZnCl_2$ [40,110,114–116] and $FeCl_3$ [117]. The chemical activation aims to increase the microporosity and surface area of biochars, and create various oxygenated functional groups that could act as proton donating exchange sites where various pollutants could be chemically adsorbed [118]. Finally, the impregnation of raw sludge with metal salts before pyrolysis has also been pointed out as a promising method producing highly efficient nano-metals-supported-biochars [118]. Indeed, the deposited metal ions from the solutions onto the surface or interior of feedstocks during the impregnation step will be converted to metal oxide nanoparticles such as MgO, MnO_2, Fe_2O_3, Al_2O_3, or zero-valent metals on the surface of the biochar. These nanoparticle-supported biochars retain various chemicals, especially those negatively charged such as P-PO_4 and N–NO_3 [92].

It is important to underline that the chemical modification of raw sludge or SDBs has mainly been applied using $ZnCl_2$ and KOH as activation agents [113–115]. These two reagents could induce significant increase in the surface area and micro-porosity of the SDBs and consequently their capacities to remove heavy metals and dyes. Fig. 2 shows the effect of various chemical modifications on SDBs surface area and their efficiencies in removing Pb(II) from aqueous solutions. It can be clearly seen that Pb(II) removal efficiency depends not only on the nature of the activating agent but also on its used concentration or dosage.

The maximal surface area ratios (modified/raw SDBs) were assessed to 11.2 and 7.9 for KOH [119] and $ZnCl_2$ [114], respectively. The KOH activation was performed through pyrolysis of the biochar mixed with KOH at a mass ratio of 1:2 (biochar-sludge/KOH) at 700 °C for 1 h. The same activation protocol with CH_3COOK resulted in a surface area increase ratio of 7.5 [119]. However, the physical activation of this material by CO_2 for 1 h at 700 °C increased its specific area by a factor of only 2.9. Lead removal efficiency increased from 7.6 (non-activated biochar) to 22.4, 47.6, and 57.5 mg g^{-1} for SDBs activated with CO_2, CH_3COOK and KOH respectively [119]. However, the activation of sludge collected from a Portuguese WWTP with $ZnCl_2$ at an equal mass ratio (1:1) followed by pyrolysis at 650 °C resulted in lower Pb(II) removal capacity (33 mg g^{-1}) [114]. For an initial pH of 5, the removal efficiencies of Hg(II) and Cu(II) by activated SDB reached relatively high values of 137.2 and 16.5 mg g^{-1} which were about 119.1%, and 358.3% greater than the ones measured for non-activated biochar. Besides, Wei et al. [115] studied the adsorption of Cu(II) by a biochar derived from an activated aerobic granular municipal sludge [115]. The collected raw sludge was firstly activated with $ZnCl_2$ (5 M) for 24 h at a dose of 400 g/L (mass ratio of 1:1.7 (raw sludge/$ZnCl_2$)) and then carbonized at 650 °C. The relatively high $ZnCl_2$ concentration resulted in a very porous SDB with a high surface area of 1175 $m^2\ g^{-1}$. For an initial pH of 5, the highest calculated adsorption capacity of Cu(II) was 18.5 mg g^{-1}, which is slightly higher than those reported by Otero et al. [114] (16.5 mg g^{-1}, Table 4) for an activated SDB with a surface area of 472 $m^2\ g^{-1}$. Lower surface area of 760 $m^2\ g^{-1}$ was obtained by Gorzin and Ghoreyshi [118] even if their SDB was generated from a pre-treated aerobically digested activated sludge of a dairy industry (Iran) with 5 M $ZnCl_2$ (mass ratio of sludge/$ZnCl_2$ = 1:3) that was pyrolyzed at 650 °C [110]. For an adsorbent dose of 3 g/L and an initial pH of 2, the adsorption capacity of Cr (VI) by this SDB was estimated to 72.8 mg g^{-1}. This adsorption capacity is about 3 times higher than an untreated biochar produced from a dewatered urban sludge at 400 °C for 2 h and having a surface area of 23.7 $m^2\ g^{-1}$ [88]. A relatively important specific surface area of an activated SDB with 5 M $ZnCl_2$ (ratio sludge/$ZnCl_2$ = 1/2.5) of 905.1 $m^2\ g^{-1}$ was reported by Ding et al. [11]. The application of this activated SDB for methylene blue (MB) removal from aqueous solutions showed high adsorption capacity (324 mg g^{-1}), which is about 13.5 times higher than the non-activated SDB [96]. Moreover, Hsiu-Mei et al. [120] studied the adsorption of Orange II dye by a $ZnCl_2$-activated SDB for 24 h in comparison with a commercial activated carbon. Even if the surface area of the SDB (737 $m^2\ g^{-1}$) was about 12.5% lower, it exhibited 52.1% higher adsorption capacity than the activated carbon. This behavior was explained by the presence on the SDB of various functional groups such as carboxylic, lactonic and phenolic groups as well as larger pore size distribution [120].

On the other hand, Lin et al. [106] compared the efficiency of SDBs produced by activation of sludge with various agents including an acid solution (H_3PO_4), an alkaline solution (KOH), and a metal salt ($ZnCl_2$) for Cu(II) and Pb(II) removal from aqueous solutions [106]. The mass ratios of reactant/sludge varied between 0.1 and 0.15 to 1. For a pyrolysis temperature of 600 °C, the measured BET surface areas and "total pore volume" were consequently relatively low (130.7, 118.3, and 104.5 $m^2\ g^{-1}$ and "0.13", "0.1" and "0.1" $cm^3\ g^{-1}$ after activation with KOH, H_3PO_4, and $ZnCl_2$, respectively). The highest Pb(II) adsorption capacity (55.9 mg g^{-1}) was observed for the SDB activated with H_3PO_4 and was mainly attributed to the introduction of more acidic functional groups (especially carboxyl) on the SDBs' surface. It is worth mentioning

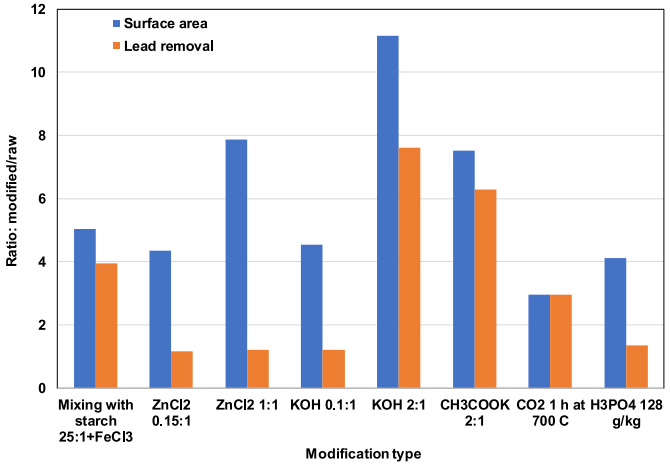

Fig. 2. Impact of the used chemical activator agent on the SDBs surface area and Pb(II) removal capacity [87,106,114,119].

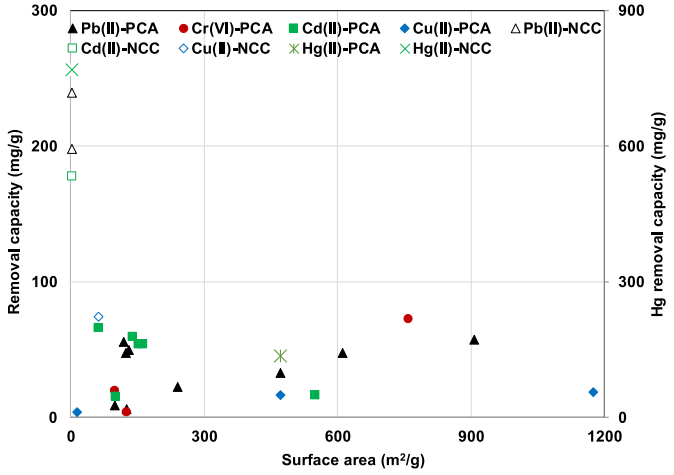

Fig. 3. Comparison between the efficiencies of SDBs treated with nano-composite coating (NCC) or physico-chemical activation (PCA) on heavy metal removal from aqueous solutions [39,83,87,92,103,110,111,114–116,119,121,122].

that even if the surface area of the H_3PO_4-activated SDB was relatively low (118.3 m^2 g^{-1}), its Pb(II) adsorption capacity was quite similar to the one assessed by Zhang et al. [119] for a KOH-activated SDB with a much higher surface area of 908 m^2 g^{-1}. It is 1.2, 1.7, and 2.5 times higher than those obtained for SDB activated with CH_3COOH [119], $ZnCl_2$ [114], and CO_2 [119] having surface areas of 611.2, 472.0, and 239.8 m^2 g^{-1}, respectively (Fig. 3). This finding confirms that Pb(II) removal by SDBs depends not only on their surface areas but also on several other parameters, including the nature and content of surface functional groups and the mineral composition.

It is worth mentioning that SDBs activation with NaOH (mass ratio of 2:1 (sludge/NaOH)) permits significant removal capacities for various pollutants (antibiotic: tetracycline (TC); pesticide: 2,4 dichlorophenol (2,4 DCP), MB dye, and Cd(II)) [39]. Indeed, even if this alkaline activation had moderately increased its specific surface area (from 47 to 139 m^2 g^{-1}) and micro-porosity (from 0.02 to 0.06 cm^3 g^{-1}), the sorption capacities of the activated SDBs reached 1249, 55, 518 and 60 mg g^{-1} for TC; 2,4 DCP, MB and Cd(II), respectively. These capacities are 4.1, 1.9, 2.5, and 1.8 times higher than those of the non-activated sludge. This increase was due to a combined effect of the biochar structure and texture improvement and the increase of basic surface functional groups content.

Conversely, HCl is generally used as a post-treatment for SDBs [2,39,112]. It appears that the efficiency of the activated SDB depends significantly on HCl concentration. As such, using 10% HCl solution to treat a biochar derived from a Mexican industrial sludge at 500 °C resulted in a specific surface area and total pore volume of 100 m^2 g^{-1} and 0.0552 cm^3 g^{-1}, respectively [111]. Consequently, this activated SDB removed only 15.1 mg g^{-1} of Cd(II) from aqueous solutions. However, the activation with 1 M HCl of paper mill SDB at 600 °C resulted in a higher surface area (194 m^2 g^{-1}), which is 14.6 times higher than the non-activated SDB [112]. The activation operation was also accompanied by a drastic decrease of CaO and MgO contents from 30.9% and 16.4% to only 0.27% and 2.89%. This activation significantly increased the MB and Procion Red MX-5B (PR) adsorption from 29.38 and 19.15 mg g^{-1} to 115.7 and 51.6 mg g^{-1}, respectively. On the other hand, the use of H_2SO_4 as a pre-treatment of raw municipal sludge (Spain) at a ratio of 1:1 followed by pyrolysis at 625 °C induced better porosity development than HCl [108]. This activation increased the surface area from 80 to 390 m^2 g^{-1}. Moreover, the adsorption capacities of crystal violet, indigo carmen and phenol increased from 184.7, 30.8, and 5.6 mg g^{-1} by 47%, 77%, and 427%, respectively [108].

Concerning nutrients, the removal efficiency of N–NH_4 from aqueous solutions seems to be highly affected by SDBs activation procedure. In this regard, Carey et al. [123] activated sludge with KOH solution (1 N) at a mass ratio sludge/KOH of 1:2.5 followed by pyrolysis at 450 °C [123]. The resultant SDB had low specific surface area (15 m^2 g^{-1}) but was about ten times more effective in removing N–NH_4 from aqueous solutions (5.3 mg g^{-1}) than a commercial activated carbon. Moreover, Yu and Zhong [40]studied the efficiency of various activated SDBs to remove P and organics from wastewaters. Three sludge of different origins were used: a biochemical sludge (BS), a surplus sludge from an urban WWTP (SS), and a biochemical sludge from the petrochemical industry (petrochemistry sludge, PS). They tested different activating agents including $ZnCl_2$, H_2SO_4, KOH and $FeSO_4$. They found that the best SDB properties were obtained by activation with a mixture of 5 M $ZnCl_2$ and 5 M H_2SO_4 with a ratio $ZnCl_2/H_2SO_4$ = 1:2 (v/v). The sludge/activating-agent ratio was fixed to 1:2.5 (m/v). The specific surface areas and the total pore volume of the SDBs generated at 550 °C of BS, SS and PS were 114.5, 144.5, and 129.0 m^2 g^{-1}; 0.07, 0.05 and 0.06 cm^3 g^{-1}, respectively. The application at a dosage of 5 g/L for the removal of COD and "P" from real wastewaters at initial concentrations of 302.4 and "19.7" mg L^{-1}, respectively reach removal efficiency yields of about 79%, 76% and 66% and "98%, 98% and 93%" for the SDBs generated from BS, PS and SS, respectively. These yields are much higher than those registered for a commercial activated carbon: 41% and 9% for COD and P, respectively.

3.1.3.2. Embedding with specific materials (biochar-based composites). Recently, SDB-based nanocomposites have been pointed out as promising adsorbents for wastewater treatment [118]. The SDB-based nanocomposites synthesis is based on combining SDB with nanomaterials to obtain metal-oxide biochars, magnetic biochars and biochars coated with nanoparticles. This procedure creates new functional groups on the SDBs surfaces that did not naturally exist on the biochar or the feedstock surface [15,118]. These surface functional groups exploit the magnetic separation capabilities, and/or catalytic properties for the degradation and treatment of various pollutants [131]. The SDB-based nanocomposites generally adsorb specific chemicals present in complex wastewater effluents such as PO_4^{3-}, NO_3^- and AsO_4^{3-}, usually negligibly retained by raw biochars [132], and can reduce specific heavy metals in stable forms such as PbO. In this context, a magnetic biochar was produced by treating a dewatered sludge with zero-valent iron (ZVI)-activated persulfate and a heating step at 600 °C in order to remove heavy metals from aqueous solutions [80]. They showed that the surface of the non-treated biochar was smooth and clean. However, the nZVI-SDB was homogeneously covered with high amounts of irregular nanoparticles (NPs) with an average dimension of 20–50 nm, which may be attributed to both nZVI and iron oxides. Compared to the raw biochar and for an initial concentration of 100 mg/L, this modification enabled the adsorption capacities of Cd(II), Pb(II), Cu(II), Ni(II), and Zn(II) to reach 33.9, 50.0, 36.8, 29.5 and 30.1 mg g^{-1}. These removal efficiencies were about 126%, 61%, 360%, 111% and 234% higher than the raw sludge, respectively. Besides, Diao et al. [87] showed that for initial Cr (VI) and Pb(II) concentrations of 30 and 15 mg/L, pH of the liquid medium of 4, a fixed dosage of 1.5 g/L of a mixture sludge/starch-derived biochar (MSSDB) at 600 °C and a MSSDB on which nanoscale zero-valent iron was immobilized (MSSDB-nZVI), these two materials removed about 30.0% and 98.8% of Cr(VI) and 40% and 91% of Pb(II), respectively. The higher removal efficiencies observed for MSSDB-nZVI compared to MSSDB were attributed to the combination of adsorption and reduction processes of Pb(II) to PbO and Cr(VI) to Cr(III), and then to Cr_2O_3 and $Cr(OH)_3$. However, the corresponding Pb(II) removal capacity (9.1 mg g^{-1}) was significantly lower than the one reported by Chen et al. [80]. It might be mainly due to the lower aqueous Pb(II) concentration and also smaller deposited amounts of ZVI on the biochars' surface. On the other hand, Chaukura et al. [117] synthesized a Fe_2O_3-biochar nano-composite from the impregnation of pulp and paper sludge by $FeCl_3$ and a pyrolysis temperature of 750 °C [117]. Despite the decrease in the surface area from 174 to 15 m^2 g^{-1}, the removal capacity of methyl orange by the nano-composite SDB was assessed to 46.6 mg g^{-1}, which is about 112% higher than the non-modified SDB. This improvement in adsorption was attributed to: i) the lower pH_{PZC} of the nano-composite SDB (2.1) compared to the non-modified SDB (8.3), and ii) the presence of higher contents of Fe on the nano-composite SDB (22.6%). Moreover, Zhang et al. [128] studied malachite green (dye) removal by a magnetized SDB synthetized by assembling strontium hexaferrite ($SrFe_{12}O_{19}$) onto the surface of the raw biochar (RB) under high temperature (800 °C) [128]. The highest malachite green adsorption capacity by this biochar was estimated to 404.9 mg g^{-1} at a mass ratio of RB and $SrFe_{12}O_{19}$ of 3:4, an adsorbent dosage of 2 g/L and a neutral pH. Moreover, Ma et al. [129] demonstrated that the combination of municipal sludge activation with $ZnCl_2$ at 500 °C and its coating with Fe/S nanoparticles efficiently removed tetracycline from aqueous solutions with an adsorption capacity of 174.1 mg g^{-1}. This capacity is three times higher than the sludge activated solely with $ZnCl_2$ [129]. The activation of the same sludge with KOH at 500 °C followed by coating with Fe/Cu nanoparticles allowed a tetracycline adsorption capacity of 387 mg g^{-1} [130]. This capacity is higher than various tested adsorbents.

On the other hand, the specific functionalization of SDB has been

considered a promising method for the removal of specific pollutants. Therefore, various coatings have been applied for SDBs [121,122]. For instance, Tang et al. [122] carried out an amino-functionalization (-NH_2) of a biochar produced from the pyrolysis of a dewatered sludge at 500 °C [122]. This modification consisted in the combination of sol-gel process for mesoporous silica coating and silylation. This amino-functionalized biochar exhibited high Cu(II) adsorption capacity (74.5 mg g^{-1}), which is two times higher than the unmodified biochar (Fig. 3). This Cu(II) removal enhancement has been imputed to the grafted amine functional groups adhered to the mesoporous silica skeleton and specifically complexed with Cu(II). Indeed, even if this modified SDB has relatively low surface area (63 m^2 g^{-1}), its Cu(II) removal capacity was about 2.6 and 2.9 higher than two $ZnCl_2$-activated SDBs having higher surface areas of 1175.1 and 472.0 m^2 g^{-1}, respectively [114,115] (Fig. 3). Furthermore, Ifthikar et al. [121] studied carboxymethyl chitosan (CMC) coating of a dewatered SDB at 400 °C [121]. They observed that the modified SDB (with a mass ratio CMC/sludge of 2:1) had relatively high C and N contents of 28.9% and 3.2%, respectively. These values were about 2.4 and 1.7 higher than the non-modified SDB. This is because CMC is a carbon skeleton polymer with an important ratio of hydroxyl and amino-functional groups. Even if modification with CMC significantly decreased the surface area and the pore volume of the SDB from about 41.0 to 2.4 m^2 g^{-1} and from 0.1164 cm^3 g^{-1} to 0.0186 cm^3 g^{-1}, the average pore width of the modified sludge (31.6 nm) was about 2.8-fold larger than the original biochar. Furthermore, the FTIR analysis of the modified SDB showed abundant functional groups such as –COOH, –OH and –NH_2 on its surface, which led to exceptional lead and mercury removal efficiency. Indeed, their adsorption capacities reached 239 and 769 mg g^{-1} for Pb (II) and Hg(II), respectively (Fig. 3).

Regarding phosphorus removal from aqueous solutions, raw SDBs exhibited low P-PO_4 adsorption capacities [40,104]. The pre-treatment of these raw sludge with materials or solutions rich in Ca and Mg allows higher P-PO_4 removal efficiencies [92,105]. Li et al. [92] demonstrated that biochar generated from the pyrolysis at 800 °C of a raw sludge mixed with dolomite (at a ratio of 1:1) permits the removal of 29 mg g^{-1} P-PO_4 (Fig. 4) [92]. This adsorption capacity increased to 153.9 mg g^{-1} (not reported in Fig. 4 because the surface area of this SDB was not assessed) when the raw anaerobically digested sludge was mixed with a synthetic solution of $CaCl_2$ and then pyrolyzed at 600 °C for 3 h [105].

3.2. Adsorption mechanisms

Identifying adsorption mechanisms is a major challenge to recognize

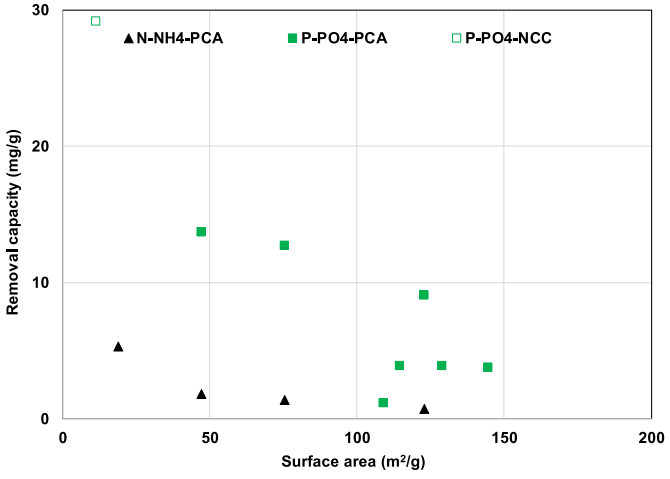

Fig. 4. Comparison between the efficiency of SDBs treatment by nano-composite coating (NCC: CaO) and physico-chemical activation (PCA) on N–NH_4 and P-PO_4 removal from aqueous solutions [40,92,93,104,105].

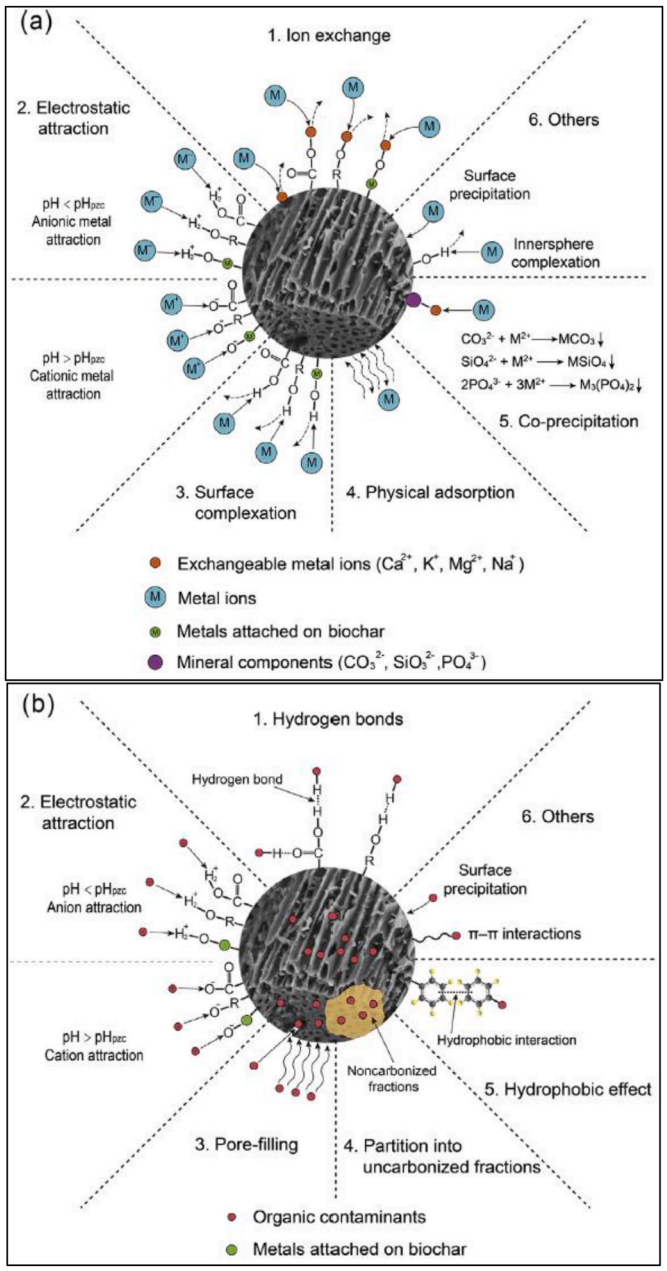

Fig. 5. A brief summary of mechanisms involved in the adsorption of toxic metals (a) and organic contaminants (b) onto biochar. Reproduced with permission from Ref. [131].

the interactions at the adsorbent/adsorbate interface [133]. It is particularly important since mechanisms identification in pollutant adsorption can facilitate the desorption process optimization [37,134]. Therefore, several studies have focused on the determination of adsorption mechanisms and different interactions have been identified. These interactions depend particularly on the adsorbent properties, pollutants nature and adsorption conditions [133]. The identified interactions include precipitation (surface precipitation), ion exchange, surface complexation with functional groups, electrostatic interactions, direct reduction (in the presence of a reductant like nZVI), hydrogen bonding, physical/chemical adsorption, etc. A visual representation of these interactions is provided in Fig. 5.

The adsorption/removal of metal ions can be associated to electrostatic attraction, surface complexation, precipitation, ion-exchange, oxidation, and reduction [37]. However, the extent of these

interactions could vary depending on the metal ion and biochar properties. For example, Lu et al. [135] demonstrated that Pb(II) sorption onto SDBs primarily involved surface complexation by organic functional groups (contributing 38–42% of the total Pb(II) sorption) and complexation by mineral components or co-precipitation releasing Ca (II) and Mg(II) (accounting for 58–62%). Similar mechanisms for Pb(II) sorption (complexation by minerals and organic functional groups, co-precipitation and/or cation exchange) have been proposed [36]. Ho et al. [81] used diverse techniques (FTIR, ICP, XRD, XPS and SEM-EDX) to explore Pb(II) adsorption mechanisms and proposed electrostatic attraction, ion exchange, surface complexation, and precipitation as the potential pathways. Biochar surface functional groups have also prominent interactions with metal ions like surface complexation, ion exchange and electrostatic interaction [58]. These interactions dictate changes in biochar structure and functional groups which are recorded by comparing biochar characteristics before and after adsorption [81]. Similarly, Iftikhar et al. [121] reported that the adsorption of Pb(II) or Hg(II) significantly shifts the characteristics FTIR bands of carboxymethyl chitosan-coated biochar due to their attachment with –COOH, $–NH_2$, and –OH functional groups evidencing the complexation and ionic bonds [121]. For Cd(II) adsorption onto municipal sewage sludge, surface precipitation of insoluble Cd compounds ($Cd(OH)_2$ (s)) in alkaline conditions and cation exchange were proposed as the major adsorption routes with a small contribution of organic functional groups [58]. The XPS findings by Zhang et al. [89] suggested that As(III) adsorption on SDBs proceeds through ligand exchange (with hydroxyl groups on biochar surface), which dominates over electrostatic interactions (based on experiments at varying pH and ionic strengths) [89].

It has also been found that biochar modification enhances its properties and adsorption capacity. For example, Zhang et al. [119] modified the biochar by physical (CO_2) and chemical (CH_3COOK or KOH) activations. They reported that activation by CH_3COOK or CO_2 improved the oxygen-containing functional groups to a greater extent compared to KOH. However, KOH activation increased the surface area of biochar and ultimately improved the Pb(II) adsorption as physical adsorption dominated. Similarly, higher adsorption of Cu(II) on amine-grafted SDBs was associated with the presence of amine group (metal-preferred ligand) that improved the tetrahedral complexation with Cu(II) [122].

Studies exploring the inclusion of nZVI (nano zero-valent iron) in biochar-based adsorbents reported metal removal enhancement while highlighting the vital role of reduction [80,87]. It should be noted that magnetic adsorbents could facilitate their recovery and reuse owing to their magnetic characteristics. Chen et al. [80] associated Pb(II) removal by magnetic biochar to the following four mechanisms: electrostatic interactions, surface complexation, ion exchange, and reduction of Pb^{2+} directly by nZVI or by Fe(II) formed from nZVI. Diao et al. [87] evaluated the use of nZVI-immobilized SDBs for simultaneous removal of Pb (II) and Cr(VI). Their findings pointed out that the role of reduction was prominent for Cr(VI) (that was reduced to Cr(III)) whereas Pb(II) was removed mainly by adsorption with little contribution of reduction. The coexistence of Pb(II) and Cd(II) in another study illustrated the competitive advantage of Pb(II) over Cd(II) because functional groups on biochar surface were preferentially occupied by Pb(II) through inner surface complexation [82] due to the higher affinity of Pb(II) [136].

Reduction (in adsorption-coupled reduction) has been proposed as the prominent mechanism for the removal of Cr(VI) based on analyses of residual Cr species (Cr(VI) and Cr(III) in aqueous solution and XPS findings [36]. It is noteworthy that adsorption mechanisms for both Cr species were reported to be different by Yuan et al. [58]. They showed that Cr(III) adsorption involved cation exchange and precipitation of Cr $(OH)_3$, whereas these two interactions were less relevant for Cr(VI). Moreover, organic functional groups showed limited contribution in adsorption of Cr(III) [58]. It should be noted that Cr(VI) can be directly reduced by its contact with the electron-donor groups of biochar and the resultant Cr(III) ions adsorb on biochar by surface complexation, ion exchange or precipitation [88]. Cr(VI) can also be indirectly reduced first by its binding to the positively-charged organic functional groups on biochar surface followed by its reduction by adjacent electron-donor groups and ultimate surface complexation of Cr(III) [88]. These authors concluded that sorption of humic acids on biochar offered additional surface sites for inner-sphere complexation and reduction.

Reaction mechanisms have been found to be different for organic pollutants. In general, organic pollutants adsorption using SDBs has been linked to various mechanisms including electrostatic interaction, hydrogen bonding, hydrophobic effect, pore filling, etc. (Fig. 5) [13,37,73,88,89,133,134]. For example, Fan et al. [96] associated the adsorption of MB with the coexistence of different mechanisms including electrostatic attraction, hydrogen bonding and interactions, and ion exchange [96]. Similarly, electrostatic attractions were proposed as the potential pathway for MB adsorption based on FTIR spectra that highlighted changes and shifting in negative carboxyl groups after pollutant adsorption on biochars derived from various sources [11]. For instance, thermal-alkaline pretreatment of sewage sludge improved the adsorption capacity of cationic red X-GRL on biochar but had a little impact on the adsorption mechanism as suggested by adsorption kinetics and isotherms [91]. Physical and chemical adsorption was confirmed, whereas chemisorption was found to be the rate-limiting step [91]. On the other hand, Tong et al. [13] showed that the involved mechanisms during micropollutants removal by SDBs depend on these pollutants' polarity. Indeed, the neutral compounds (17 β-estradiol, 17 α-ethynylestradiol, and triclosan) were mainly removed through hydrophobic interactions. However, polar contaminants such as benzyldimethyldecylammonium chloride and carbamazepine were mainly removed through weak interactions with the more polar amorphous moieties on the SDBs surface.

4. Conclusions and future research directions

This review proves that sewage sludge is a promising feedstock for producing efficient and cost-effective biochars to treat both urban and industrial wastewaters. This efficiency is intimately linked to the sludge's nature and the SDBs physico-chemical properties, which are very dependent on synthesis conditions. Due to their intrinsic composition, the digested sludge-derived biochars exhibit better nutrients and heavy metals adsorption capacities than the non-digested ones. These nutrient recovery efficiencies could be significantly improved if the raw sludge is mixed with lignocellulosic biomasses, especially natural Mg/Ca rich materials such as dolomite.

For high removal efficiencies, the pyrolysis conditions of sludge should be meticulously chosen depending on the nature and properties of target pollutants. Indeed, besides the specific surface area and microporosity development, the presence of specific nanomaterials and adapted functional groups on the surface of the SDBs can be of great interest. In general, the higher is the pyrolysis temperature, the better are SDBs physico-chemical characteristics and ultimate sorption properties. However, to acquire more important adsorption capacities for various organic and inorganic pollutants, physical and chemical modification are highly rewarding. In contrast to physical activation, the chemical activation of sludge by using specific alkali metals hydroxide reagents (KOH), metal salts ($ZnCl_2$) and acids (H_3PO_4) is very effective in producing SDBs with distinguished physico-chemical characteristics. For chemical reagents/sludge ratios >2:1, the modified SDBs exhibit higher adsorption capacities for both inorganic and organic pollutants compared to several commercial activated carbons. For specific toxic pollutants such as dyes, heavy metals, and oxyanions, the related removal efficiencies could be significantly improved through the embedment/coating of SDBs with specific nanomaterials and tailored functional groups. Some SDB-based nanocomposites (e.g. magnetite SDBs) are efficient for toxic pollutants adsorption and could enhance their degradation and chemical reduction.

Different research avenues regarding SDBs valorization as effective and low-cost adsorbents for urban and industrial wastewater treatment

should be explored in the future. These perspectives have to address:

- The operating conditions optimization of the non-modified SDBs generated from the pyrolysis of raw and mixed sludge with Fe/Ca/Mg materials during urban wastewater treatment. The main goal is to recover the contained nutrients (especially nitrogen, phosphorus and potassium) and to safely valorize these nutrient-enriched SDBs in agriculture. In this context, monitoring the release of these nutrients and undesirable compounds from these SDBs under different experimental conditions is urgently required. Understanding their effect on the physico-chemical, biological and hydrodynamic characteristics of amended soils and on plant growth would be of great interest.
- The achievement of cost-effective modified SDBs for an efficient removal of both mineral and organic compounds from wastewater. In this context, two options should be explored. The first one is optimizing the sludge physico-chemical activation using a mixture of reagents, depending on the targeted pollutants. The second option concerns the exploitation of the high surface areas of raw SDBs to embed nano-composites. The adsorption process optimization by these modified SDBs should be performed by using innovative approaches such as the "response surface methodology (RSM)".
- Exploiting the efficient SDBs use for pollutants removal from real effluents under dynamic conditions using laboratory columns and/or continuously renewed tank reactors. During these dynamic investigations, it is essential to accurately assess the role of several parameters such as the residence time, the bed depth height of the raw/mixed SDBs with other materials, and the quality of the wastewater under realistic conditions. The numerical modeling with adapted empirical solutions and existing models for the prediction of pollutant breakthrough curves would contribute to the optimization of the dynamic adsorption process for an easy system up scaling.
- A better assessment of the competitive sorption of various inorganic and organic pollutants in co-contaminated solutions using SDBs as adsorbents. The assessment of the competitive sorption of various organic/mineral pollutants contained in real urban or industrial wastewaters in the presence of, for instance, humic acids and organic matter is required.
- The implementation of a sustainable management strategy for pollutant-loaded SDBs is crucial. This strategy should obey the circular economy concept and will permit: i) an eco-friendly and low-cost regeneration and reuse of these SDBs in future adsorption cycles, ii) the recovery of the adsorbed chemicals and their reuse in industry as resources, and iii) the preservation of the environment against pollution.

Finally, it is essential to reduce the energetic production cost of SDBs during the pyrolysis process through bio-oil and syngas valorization in the production plant. This energy economy will favor the widespread acceptance of this thermochemical conversion technology.

Declaration of competing interest

The authors declare that they have no known competing financial interests or personal relationships that could have appeared to influence the work reported in this paper.

Acknowledgements

S.J., M.U., and Y.C. would like to gratefully acknowledge the Madayn, Oman for its financial support. B.K., H.H., and M.J. thank the support provided by CERTE (Tunisia), QU (Qatar), and IS2M (France) respectively.

Appendix A. Supplementary data

Supplementary data to this article can be found online at https://doi.org/10.1016/j.rser.2021.111068.

References

[1] Nations United. World population prospects 2019: highlights. United Nations Publ; 2019. https://population.un.org/wpp/Publications/Files/WPP2019_Highlights.pdf.
[2] Gherghel A, Teodosiu C, De Gisi S. A review on wastewater sludge valorisation and its challenges in the context of circular economy. J Clean Prod 2019;228:244–63.
[3] Seleiman MF, Santanen A, Mäkelä PSA. Recycling sludge on cropland as fertilizer – advantages and risks. Resour Conserv Recycl 2020;155:104647.
[4] Hamdi H, Hechmi S, Khelil MN, Zoghlami IR, Benzarti S, Mokni-Tlili S, et al. Repetitive land application of urban sewage sludge: effect of amendment rates and soil texture on fertility and degradation parameters. Catena 2019;172:11–20.
[5] Kor-Bicakci G, Eskicioglu C. Recent developments on thermal municipal sludge pretreatment technologies for enhanced anaerobic digestion. Renew Sustain Energy Rev 2019;110:423–43.
[6] Chang Z, Long G, Zhou JL, Ma C. Valorization of sewage sludge in the fabrication of construction and building materials: a review. Resources,. Conserv Recycl 2020;154:104606.
[7] Raheem A, Sikarwar VS, He J, Dastyar W, Dionysiou DD, Wang W, et al. Opportunities and challenges in sustainable treatment and resource reuse of sewage sludge: a review. Chem Eng J 2018;337:616–41.
[8] Liu Z, McNamara P, Zitomer D. Autocatalytic pyrolysis of wastewater biosolids for product upgrading. Environ Sci Technol 2017;51:9808–16.
[9] Breulmann M, Schulz E, van Afferden M, Müller RA, Fühner C. Hydrochars derived from sewage sludge: effects of pre-treatment with water on char properties, phytotoxicity and chemical structure. Arch Agron Soil Sci 2018;64:860–72.
[10] Liu Z, Singer S, Tong Y, Kimbell L, Anderson E, Hughes M, et al. Characteristics and applications of biochars derived from wastewater solids. Renew Sustain Energy Rev 2018;90:650–64.
[11] Ding X, Chen H, Yang Q, Wei J, Wei D. Effect of sludge property on the synthesis, characterization and sorption performance of sludge-based biochar. Bioresour Technol Rep 2019;7:100204.
[12] Yao Y, Gao B, Inyang M, Zimmerman AR, Cao X, Pullammanappallil P, et al. Biochar derived from anaerobically digested sugar beet tailings: characterization and phosphate removal potential. Bioresour Technol 2011;102:6273–8.
[13] Tong Y, Mayer BK, McNamara PJ. Adsorption of organic micropollutants to biosolids-derived biochar: estimation of thermodynamic parameters. Environ Sci: Water Res Technol 2019;5:1132–44.
[14] Tong Y, Mayer BK, McNamara PJ. Triclosan adsorption using wastewater biosolids-derived biochar. Environ Sci: Water Res Technol 2016;2:761–8.
[15] Qambrani NA, Rahman MM, Won S, Shim S, Ra C. Biochar properties and eco-friendly applications for climate change mitigation, waste management, and wastewater treatment: a review. Renew Sustain Energy Rev 2017;79:255–73.
[16] Andreoli CV, von Sperling M, Fernandes F. Sludge Treat Disposal: IWA Publ 2007.
[17] Brahmi M, Belhadi NH, Hamdi H, Hassen A. Modeling of secondary treated wastewater disinfection by UV irradiation: effects of suspended solids content. J Environ Sci 2010;22:1218–24.
[18] Atinkpahoun CNH, Le ND, Pontvianne S, Poirot H, Leclerc JP, Pons MN, et al. Population mobility and urban wastewater dynamics. Sci Total Environ 2018;622–623:1431–7.
[19] Kumar V, Chopra AK, Kumar A. A review on sewage sludge (Biosolids) a resource for sustainable agriculture. Arch Agric Environ Sci 2017;2:340–7.
[20] Rehman RA, Rizwan M, Qayyum MF, Ali S, Zia-ur-Rehman M, Zafar-ul-Hye M, et al. Efficiency of various sewage sludges and their biochars in improving selected soil properties and growth of wheat (Triticum aestivum). J Environ Manag 2018;223:607–13.
[21] Hechmi S, Hamdi H, Mokni-Tlili S, Zoghlami IR, Khelil MN, Benzarti S, et al. Carbon mineralization, biological indicators, and phytotoxicity to assess the impact of urban sewage sludge on two light-textured soils in a microcosm. J Environ Qual 2020;49:460–71.
[22] Du W, Jiang J, Gong C. Primary research on agricultural effect of sludge–impact of sludge application on crop seeds germination and seedling growth. Procedia Environ Sci 2012;16:340–5.
[23] Gu C, Bai Y, Tao T, Chen G, Shan Y. Effect of sewage sludge amendment on heavy metal uptake and yield of ryegrass seedling in a mudflat soil. J Environ Qual 2013;42:421–8.
[24] Mahmoud FS, Shaimaa S, Seija J, Pirjo SAM. Chemical composition and in vitro digestibility of whole-crop maize fertilized with synthetic fertilizer or digestate and harvested at two maturity stages in Boreal growing conditions. Agric Food Sci 2017:26.
[25] Singh RP, Agrawal M. Potential benefits and risks of land application of sewage sludge. Waste Manag 2008;28:347–58.
[26] Hamdi H, Benzarti S, Manusadzianas L, Aoyama I, Jedidi N. Solid-phase bioassays and soil microbial activities to evaluate PAH-spiked soil ecotoxicity after a long-term bioremediation process simulating landfarming. Chemosphere 2007;70:135–43.
[27] Miller-Robbie L, Ulrich BA, Ramey DF, Spencer KS, Herzog SP, Cath TY, et al. Life cycle energy and greenhouse gas assessment of the co-production of biosolids and biochar for land application. J Clean Prod 2015;91:118–27.
[28] Paz-Ferreiro J, Nieto A, Méndez A, Askeland MPJ, Gascó G. Biochar from biosolids pyrolysis: a review. Int J Environ Res Publ Health 2018;15:956.

[29] Khiari B, Jeguirim M, Limousy L, Bennici S. Biomass derived chars for energy applications. Renew Sustain Energy Rev 2019;108:253–73.
[30] Tasca AL, Puccini M, Gori R, Corsi I, Galletti AMR, Vitolo S. Hydrothermal carbonization of sewage sludge: a critical analysis of process severity, hydrochar properties and environmental implications. Waste Manag 2019;93:1–13.
[31] Azzaz AA, Khiari B, Jellali S, Ghimbeu CM, Jeguirim M. Hydrochars production, characterization and application for wastewater treatment: a review. Renew Sustain Energy Rev 2020;127:109882.
[32] Cha JS, Choi J-C, Ko JH, Park Y-K, Park SH, Jeong K-E, et al. The low-temperature SCR of NO over rice straw and sewage sludge derived char. Chem Eng J 2010;156:321–7.
[33] Cha JS, Park SH, Jung S-C, Ryu C, Jeon J-K, Shin M-C, et al. Production and utilization of biochar: a review. J Ind Eng Chem 2016;40:1–15.
[34] Crombie K, Mašek O. Investigating the potential for a self-sustaining slow pyrolysis system under varying operating conditions. Bioresour Technol 2014;162:148–56.
[35] Li D-C, Jiang H. The thermochemical conversion of non-lignocellulosic biomass to form biochar: a review on characterizations and mechanism elucidation. Bioresour Technol 2017;246:57–68.
[36] Zhang W, Mao S, Chen H, Huang L, Qiu R. Pb(II) and Cr(VI) sorption by biochars pyrolyzed from the municipal wastewater sludge under different heating conditions. Bioresour Technol 2013;147:545–52.
[37] Alvarez J, Amutio M, Lopez G, Barbarias I, Bilbao J, Olazar M. Sewage sludge valorization by flash pyrolysis in a conical spouted bed reactor. Chem Eng J 2015;273:173–83.
[38] Puig-Gamero M, Fernandez-Lopez M, Sánchez P, Valverde JL, Sanchez-Silva L. Pyrolysis process using a bench scale high pressure thermobalance. Fuel Process Technol 2017;167:345–54.
[39] Gómez-Pacheco CV, Rivera-Utrilla J, Sánchez-Polo M, López-Peñalver JJ. Optimization of the preparation process of biological sludge adsorbents for application in water treatment. J Hazard Mater 2012;217–218:76–84.
[40] Yu L, Zhong Q. Preparation of adsorbents made from sewage sludges for adsorption of organic materials from wastewater. J Hazard Mater 2006;137:359–66.
[41] Chun YN, Ji DW, Yoshikawa K. Pyrolysis and gasification characterization of sewage sludge for high quality gas and char production. J Mech Sci Technol 2013;27:263–72.
[42] You S, Ok YS, Tsang DCW, Kwon EE, Wang C-H. Towards practical application of gasification: a critical review from syngas and biochar perspectives. Crit Rev Environ Sci Technol 2018;48:1165–213.
[43] Zhai Y, Liu X, Zhu Y, Peng C, Wang T, Zhu L, et al. Hydrothermal carbonization of sewage sludge: the effect of feed-water pH on fate and risk of heavy metals in hydrochars. Bioresour Technol 2016;218:183–8.
[44] Zhang Z, Zhu Z, Shen B, Liu L. Insights into biochar and hydrochar production and applications: a review. Energy 2019;171:581–98.
[45] Zhu L, Lei H, Zhang Y, Zhang X, Bu Q, Wei Y, et al. A review of biochar derived from pyrolysis and its application in biofuel production. SF J Mat Chem Eng 2018:1.
[46] Domínguez A, Fernández Y, Fidalgo B, Pis JJ, Menéndez JA. Bio-syngas production with low concentrations of CO2 and CH4 from microwave-induced pyrolysis of wet and dried sewage sludge. Chemosphere 2008;70:397–403.
[47] Liu T, Guo Y, Peng N, Lang Q, Xia Y, Gai C, et al. Nitrogen transformation among char, tar and gas during pyrolysis of sewage sludge and corresponding hydrochar. J Anal Appl Pyrol 2017;126:298–306.
[48] Tripathi M, Sahu JN, Ganesan P. Effect of process parameters on production of biochar from biomass waste through pyrolysis: a review. Renew Sustain Energy Rev 2016;55:467–81.
[49] Trinh TN, Jensen PA, Dam-Johansen K, Knudsen NO, Sørensen HR. Influence of the pyrolysis temperature on sewage sludge product distribution, bio-oil, and char properties. Energy Fuel 2013;27:1419–27.
[50] Shao J, Yan R, Chen H, Wang B, Lee DH, Liang DT. Pyrolysis characteristics and kinetics of sewage sludge by thermogravimetry fourier transform infrared analysis. Energy Fuel 2008;22:38–45.
[51] Liu C, Tang Z, Chen Y, Su S, Jiang W. Characterization of mesoporous activated carbons prepared by pyrolysis of sewage sludge with pyrolusite. Bioresour Technol 2010;101:1097–101.
[52] Hossain MK, Strezov V, Nelson PF. Thermal characterisation of the products of wastewater sludge pyrolysis. J Anal Appl Pyrol 2009;85:442–6.
[53] Bagreev A, Bandosz TJ, Locke DC. Pore structure and surface chemistry of adsorbents obtained by pyrolysis of sewage sludge-derived fertilizer. Carbon 2001;39:1971–9.
[54] Belhachemi M, Khiari B, Jeguirim M, Sepúlveda-Escribano A. 3-Characterization of biomass-derived chars. In: Jeguirim M, Limousy L, editors. Char and carbon materials derived from biomass. Elsevier; 2019. p. 69–108.
[55] Moreira MT, Noya I, Feijoo G. The prospective use of biochar as adsorption matrix – a review from a lifecycle perspective. Bioresour Technol 2017;246:135–41.
[56] Agrafioti E, Bouras G, Kalderis D, Diamadopoulos E. Biochar production by sewage sludge pyrolysis. J Anal Appl Pyrol 2013;101:72–8.
[57] Bridle TR, Pritchard D. Energy and nutrient recovery from sewage sludge via pyrolysis. Water Sci Technol 2004;50:169–75.
[58] Yuan H, Lu T, Huang H, Zhao D, Kobayashi N, Chen Y. Influence of pyrolysis temperature on physical and chemical properties of biochar made from sewage sludge. J Anal Appl Pyrol 2015;112:284–9.
[59] Chen H, Zhou Y, Zhao H, Li Q. A comparative study on behavior of heavy metals in pyrochar and hydrochar from sewage sludge. Energy Sources, Part A: Recov Util Environ Effects 2018;40:565–71.
[60] Hwang IH, Ouchi Y, Matsuto T. Characteristics of leachate from pyrolysis residue of sewage sludge. Chemosphere 2007;68:1913–9.
[61] Wang J, Wang S. Preparation, modification and environmental application of biochar: a review. J Clean Prod 2019;227:1002–22.
[62] Wakkel M, Khiari B, Zagrouba F. Textile wastewater treatment by agro-industrial waste: equilibrium modelling, thermodynamics and mass transfer mechanisms of cationic dyes adsorption onto low-cost lignocellulosic adsorbent. J Taiwan Instit Chem Eng 2019;96:439–52.
[63] Wakkel M, Khiari B, Zagrouba F. Basic red 2 and methyl violet adsorption by date pits: adsorbent characterization, optimization by RSM and CCD, equilibrium and kinetic studies. Environ Sci Pollut Control Ser 2019;26:18942–60.
[64] Lu T, Yuan HR, Zhou SG, Huang HY, Noriyuki K, Chen Y. On the pyrolysis of sewage sludge: the influence of pyrolysis temperature on biochar, liquid and gas fractions. Adv Mater Res 2012;518–523:3412–20.
[65] Zielińska A, Oleszczuk P. Effect of pyrolysis temperatures on freely dissolved polycyclic aromatic hydrocarbon (PAH) concentrations in sewage sludge-derived biochars. Chemosphere 2016;153:68–74.
[66] Ábrego J, Arauzo J, Sánchez JL, Gonzalo A, Cordero T, Rodríguez-Mirasol J. Structural changes of sewage sludge char during fixed-bed pyrolysis. Ind Eng Chem Res 2009;48:3211–21.
[67] Zou J, Dai Y, Wang X, Ren Z, Tian C, Pan K, et al. Structure and adsorption properties of sewage sludge-derived carbon with removal of inorganic impurities and high porosity. Bioresour Technol 2013;142:209–17.
[68] Buah WK, Cunliffe AM, Williams PT. Characterization of products from the pyrolysis of municipal solid waste. Process Saf Environ Protect 2007;85:450–7.
[69] Pietrzak R, Bandosz TJ. Reactive adsorption of NO2 at dry conditions on sewage sludge-derived materials. Environ Sci Technol 2007;41:7516–22.
[70] Smith KM, Fowler GD, Pullket S, Graham NJD. Sewage sludge-based adsorbents: a review of their production, properties and use in water treatment applications. Water Res 2009;43:2569–94.
[71] Regkouzas P, Diamadopoulos E. Adsorption of selected organic micro-pollutants on sewage sludge biochar. Chemosphere 2019;224:840–51.
[72] Wang Z, Liu K, Xie L, Zhu H, Ji S, Shu X. Effects of residence time on characteristics of biochars prepared via co-pyrolysis of sewage sludge and cotton stalks. J Anal Appl Pyrol 2019;142:104659.
[73] Dai Q, Jiang X, Lv G, Ma X, Jin Y, Wang F, et al. Investigation into particle size influence on PAH formation during dry sewage sludge pyrolysis: TG-FTIR analysis and batch scale research. J Anal Appl Pyrol 2015;112:388–93.
[74] Lu H, Zhang W, Wang S, Zhuang L, Yang Y, Qiu R. Characterization of sewage sludge-derived biochars from different feedstocks and pyrolysis temperatures. J Anal Appl Pyrol 2013;102:137–43.
[75] Racek J, Sevcik J, Chorazy T, Kucerik J, Hlavinek P. Biochar – recovery material from pyrolysis of sewage sludge: a review. Waste Biomass Valor 2019.
[76] Rosales E, Meijide J, Pazos M, Sanromán MA. Challenges and recent advances in biochar as low-cost biosorbent: from batch assays to continuous-flow systems. Bioresour Technol 2017;246:176–92.
[77] Wei H, Gao B, Ren J, Li A, Yang H. Coagulation/flocculation in dewatering of sludge: a review. Water Res 2018;143:608–31.
[78] Lu GQ. Effect of pre-drying on the pore structure development of sewage sludge during pyrolysis. Environ Technol 1995;16:495–9.
[79] McNamara PJ, Koch JD, Liu Z, Zitomer DH. Pyrolysis of dried wastewater biosolids can Be energy positive. Water environment research. Res Publ Water Environ Feder 2016;88:804–10.
[80] Y-d Chen, Ho S-H, Wang D, Wei Z-s, Chang J-S, Ren N-q. Lead removal by a magnetic biochar derived from persulfate-ZVI treated sludge together with one-pot pyrolysis. Bioresour Technol 2018;247:463–70.
[81] Ho S-H, Chen Y-d, Yang Z-k, Nagarajan D, Chang J-S, Ren N-q. High-efficiency removal of lead from wastewater by biochar derived from anaerobic digestion sludge. Bioresour Technol 2017;246:142–9.
[82] Ni B-J, Huang Q-S, Wang C, Ni T-Y, Sun J, Wei W. Competitive adsorption of heavy metals in aqueous solution onto biochar derived from anaerobically digested sludge. Chemosphere 2019;219:351–7.
[83] Velghe I, Carleer R, Yperman J, Schreurs S, D'Haen J. Characterisation of adsorbents prepared by pyrolysis of sludge and sludge/disposal filter cake mix. Water Res 2012;46:2783–94.
[84] Chen T, Zhou Z, Xu S, Wang H, Lu W. Adsorption behavior comparison of trivalent and hexavalent chromium on biochar derived from municipal sludge. Bioresour Technol 2015;190:388–94.
[85] Chen T, Zhou Z, Han R, Meng R, Wang H, Lu W. Adsorption of cadmium by biochar derived from municipal sewage sludge: impact factors and adsorption mechanism. Chemosphere 2015;134:286–93.
[86] Chen T, Zhang Y, Wang H, Lu W, Zhou Z, Zhang Y, et al. Influence of pyrolysis temperature on characteristics and heavy metal adsorptive performance of biochar derived from municipal sewage sludge. Bioresour Technol 2014;164:47–54.
[87] Diao Z-H, Du J-J, Jiang D, Kong L-J, Huo W-Y, Liu C-M, et al. Insights into the simultaneous removal of Cr6+ and Pb2+ by a novel sewage sludge-derived biochar immobilized nanoscale zero valent iron: coexistence effect and mechanism. Sci Total Environ 2018;642:505–15.
[88] Zhou F, Wang H, Se Fang, Zhang W, Qiu R. Pb(II), Cr(VI) and atrazine sorption behavior on sludge-derived biochar: role of humic acids. Environ Sci Pollut Control Ser 2015;22:16031–9.
[89] Zhang W, Zheng J, Zheng P, Tsang DCW, Qiu R. Sludge-derived biochar for arsenic(III) immobilization: effects of solution chemistry on sorption behavior. J Environ Qual 2015;44:1119–26.

[90] Agrafioti E, Kalderis D, Diamadopoulos E. Arsenic and chromium removal from water using biochars derived from rice husk, organic solid wastes and sewage sludge. J Environ Manag 2014;133:309–14.
[91] Shen T, Tang Y, Lu X-Y, Meng Z. Mechanisms of copper stabilization by mineral constituents in sewage sludge biochar. J Clean Prod 2018;193:185–93.
[92] Li J, Li B, Huang H, Lv X, Zhao N, Guo G, et al. Removal of phosphate from aqueous solution by dolomite-modified biochar derived from urban dewatered sewage sludge. Sci Total Environ 2019;687:460–9.
[93] Yin Q, Liu M, Ren H. Biochar produced from the co-pyrolysis of sewage sludge and walnut shell for ammonium and phosphate adsorption from water. J Environ Manag 2019;249:109410.
[94] Tang Y, Alam MS, Konhauser KO, Alessi DS, Xu S, Tian W, et al. Influence of pyrolysis temperature on production of digested sludge biochar and its application for ammonium removal from municipal wastewater. J Clean Prod 2019;209:927–36.
[95] Chen S, Qin C, Wang T, Chen F, Li X, Hou H, et al. Study on the adsorption of dyestuffs with different properties by sludge-rice husk biochar: adsorption capacity, isotherm, kinetic, thermodynamics and mechanism. J Mol Liq 2019; 285:62–74.
[96] Fan S, Wang Y, Wang Z, Tang J, Tang J, Li X. Removal of methylene blue from aqueous solution by sewage sludge-derived biochar: adsorption kinetics, equilibrium, thermodynamics and mechanism. J Environ Chem Eng 2017;5: 601–11.
[97] Jindarom C, Meeyoo V, Kitiyanan B, Rirksomboon T, Rangsunvigit P. Surface characterization and dye adsorptive capacities of char obtained from pyrolysis/ gasification of sewage sludge. Chem Eng J 2007;133:239–46.
[98] Kalderis D, Kayan B, Akay S, Kulaksız E, Gözmen B. Adsorption of 2,4-dichlorophenol on paper sludge/wheat husk biochar: process optimization and comparison with biochars prepared from wood chips, sewage sludge and hog fuel/demolition waste. J Environ Chem Eng 2017;5:2222–31.
[99] Devi P, Saroha AK. Effect of pyrolysis temperature on polycyclic aromatic hydrocarbons toxicity and sorption behaviour of biochars prepared by pyrolysis of paper mill effluent treatment plant sludge. Bioresour Technol 2015;192: 312–20.
[100] Inyang M, Gao B, Yao Y, Xue Y, Zimmerman AR, Pullammanappallil P, et al. Removal of heavy metals from aqueous solution by biochars derived from anaerobically digested biomass. Bioresour Technol 2012;110:50–6.
[101] Méndez A, Gascó G, Freitas MMA, Siebielec G, Stuczynski T, Figueiredo JL. Preparation of carbon-based adsorbents from pyrolysis and air activation of sewage sludges. Chem Eng J 2005;108:169–77.
[102] Nielsen L, Zhang P, Bandosz TJ. Adsorption of carbamazepine on sludge/fish waste derived adsorbents: effect of surface chemistry and texture. Chem Eng J 2015;267:170–81.
[103] Xue Y, Wang C, Hu Z, Zhou Y, Xiao Y, Wang T. Pyrolysis of sewage sludge by electromagnetic induction: biochar properties and application in adsorption removal of Pb(II), Cd(II) from aqueous solution. Waste Manag 2019;89:48–56.
[104] Melia PM, Busquets R, Hooda PS, Cundy AB, Sohi SP. Driving forces and barriers in the removal of phosphorus from water using crop residue, wood and sewage sludge derived biochars. Sci Total Environ 2019;675:623–31.
[105] Saadat S, Raei E, Talebbeydokhti N. Enhanced removal of phosphate from aqueous solutions using a modified sludge derived biochar: comparative study of various modifying cations and RSM based optimization of pyrolysis parameters. J Environ Manag 2018;225:75–83.
[106] Lin QH, Cheng H, Chen GY. Preparation and characterization of carbonaceous adsorbents from sewage sludge using a pilot-scale microwave heating equipment. J Anal Appl Pyrol 2012;93:113–9.
[107] Gascó G, Méndez A, Gascó JM. Preparation of carbon-based adsorbents from sewage sludge pyrolysis to remove metals from water. Desalination 2005;180: 245–51.
[108] Otero M, Rozada F, Calvo LF, García AI, Morán A. Elimination of organic water pollutants using adsorbents obtained from sewage sludge. Dyes Pigments 2003; 57:55–65.
[109] Xi X, Guo X. Preparation of bio-charcoal from sewage sludge and its performance on removal of Cr (VI) from aqueous solutions. J Mol Liq 2013;183:26–30.
[110] Gorzin F, Ghoreyshi AA. Synthesis of a new low-cost activated carbon from activated sludge for the removal of Cr (VI) from aqueous solution: equilibrium, kinetics, thermodynamics and desorption studies. Kor J Chem Eng 2013;30: 1594–602.
[111] Gutiérrez-Segura E, Solache-Ríos M, Colín-Cruz A, Fall C. Adsorption of cadmium by Na and Fe modified zeolitic tuffs and carbonaceous material from pyrolyzed sewage sludge. J Environ Manag 2012;97:6–13.
[112] Hu S-H, Hu S-C. Kinetics of ionic dyes adsorption with magnetic-modified sewage sludge. Environ Prog Sustain Energy 2014;33:905–12.
[113] Kaçan E, Kütahyalı C. Adsorption of strontium from aqueous solution using activated carbon produced from textile sewage sludges. J Anal Appl Pyrol 2012; 97:149–57.
[114] Otero M, Rozada F, Morán A, Calvo LF, García AI. Removal of heavy metals from aqueous solution by sewage sludge based sorbents: competitive effects. Desalination 2009;239:46–57.
[115] Wei D, Ngo HH, Guo W, Xu W, Du B, Khan MS, et al. Biosorption performance evaluation of heavy metal onto aerobic granular sludge-derived biochar in the presence of effluent organic matter via batch and fluorescence approaches. Bioresour Technol 2018;249:410–6.
[116] Zhai Y, Wei X, Zeng G, Zhang D, Chu K. Study of adsorbent derived from sewage sludge for the removal of Cd2+, Ni2+ in aqueous solutions. Separ Purif Technol 2004;38:191–6.
[117] Chaukura N, Murimba EC, Gwenzi W. Synthesis, characterisation and methyl orange adsorption capacity of ferric oxide–biochar nano-composites derived from pulp and paper sludge. Appl Water Sci 2017;7:2175–86.
[118] Liu Y, Ran C, Siddiqui AR, Siyal AA, Song Y, Dai J, et al. Characterization and analysis of sludge char prepared from bench-scale fluidized bed pyrolysis of sewage sludge. Energy 2020;200:117398.
[119] Zhang J, Shao J, Jin Q, Li Z, Zhang X, Chen Y, et al. Sludge-based biochar activation to enhance Pb(II) adsorption. Fuel 2019;252:101–8.
[120] Hsiu-Mei C, Ting-Chien C, San-De P, Chiang H-L. Adsorption characteristics of Orange II and Chrysophenine on sludge adsorbent and activated carbon fibers. J Hazard Mater 2009;161:1384–90.
[121] Ifthikar J, Jiao X, Ngambia A, Wang T, Khan A, Jawad A, et al. Facile one-pot synthesis of sustainable carboxymethyl chitosan – sewage sludge biochar for effective heavy metal chelation and regeneration. Bioresour Technol 2018;262: 22–31.
[122] Tang S, Shao N, Zheng C, Yan F, Zhang Z. Amino-functionalized sewage sludge-derived biochar as sustainable efficient adsorbent for Cu(II) removal. Waste Manag 2019;90:17–28.
[123] Carey DE, McNamara PJ, Zitomer DH. Biochar from pyrolysis of biosolids for nutrient adsorption and turfgrass cultivation. Water Environ Res 2015;87: 2098–106.
[124] Jaria G, Calisto V, Gil MV, Otero M, Esteves VI. Removal of fluoxetine from water by adsorbent materials produced from paper mill sludge. J Colloid Interface Sci 2015;448:32–40.
[125] Kong L, Xiong Y, Sun L, Tian S, Xu X, Zhao C, et al. Sorption performance and mechanism of a sludge-derived char as porous carbon-based hybrid adsorbent for benzene derivatives in aqueous solution. J Hazard Mater 2014;274:205–11.
[126] Xiao B, Dai Q, Yu X, Yu P, Zhai S, Liu R, et al. Effects of sludge thermal-alkaline pretreatment on cationic red X-GRL adsorption onto pyrolysis biochar of sewage sludge. J Hazard Mater 2018;343:347–55.
[127] Gutiérrez-Segura E, Solache-Ríos M, Colín-Cruz A. Sorption of indigo carmine by a Fe-zeolitic tuff and carbonaceous material from pyrolyzed sewage sludge. J Hazard Mater 2009;170:1227–35.
[128] Zhang J, Liu M, Yang T, Yang K, Wang H. A novel magnetic biochar from sewage sludge: synthesis and its application for the removal of malachite green from wastewater. Water science and technology : J Int Assoc Water Pollut Res 2016;74: 1971–9.
[129] Ma J, Zhou B, Zhang H, Zhang W. Fe/S modified sludge-based biochar for tetracycline removal from water. Powder Technol 2020;364:889–900.
[130] Ma J, Zhou B, Zhang H, Zhang W, Wang Z. Activated municipal wasted J Int Assoc Water Pollut Resbiochar supported by nanoscale Fe/Cu composites for tetracycline removal from water. Chem Eng Res Des 2019;149:209–19.
[131] Tan X, Liu Y, Zeng G, Wang X, Hu X, Gu Y, et al. Application of biochar for the removal of pollutants from aqueous solutions. Chemosphere 2015;125:70–85.
[132] Haddad K, Jellali S, Jeguirim M. Ben Hassen Trabelsi A, Limousy L. Investigations on phosphorus recovery from aqueous solutions by biochars derived from magnesium-pretreated cypress sawdust. J Environ Manag 2018;216:305–14.
[133] Tong Y, McNamara PJ, Mayer BK. Adsorption of organic micropollutants onto biochar: a review of relevant kinetics, mechanisms and equilibrium. Environ Sci: Water Res Technol 2019;5:821–38.
[134] Zhang C, Zeng G, Huang D, Lai C, Chen M, Cheng M, et al. Biochar for environmental management: mitigating greenhouse gas emissions, contaminant treatment, and potential negative impacts. Chem Eng J 2019;373:902–22.
[135] Lu H, Zhang W, Yang Y, Huang X, Wang S, Qiu R. Relative distribution of Pb2+ sorption mechanisms by sludge-derived biochar. Water Res 2012;46:854–62.
[136] Ajmal Z, Usman M, Anastopoulos I, Qadeer A, Zhu R, Wakeel A, et al. Use of nano-/micro-magnetite for abatement of cadmium and lead contamination. J Environ Manag 2020;264:110477.